STUDENT REPORT AALBORG UNIVERSITY

Synchronous and zero sequence impedance in a 60kV power system

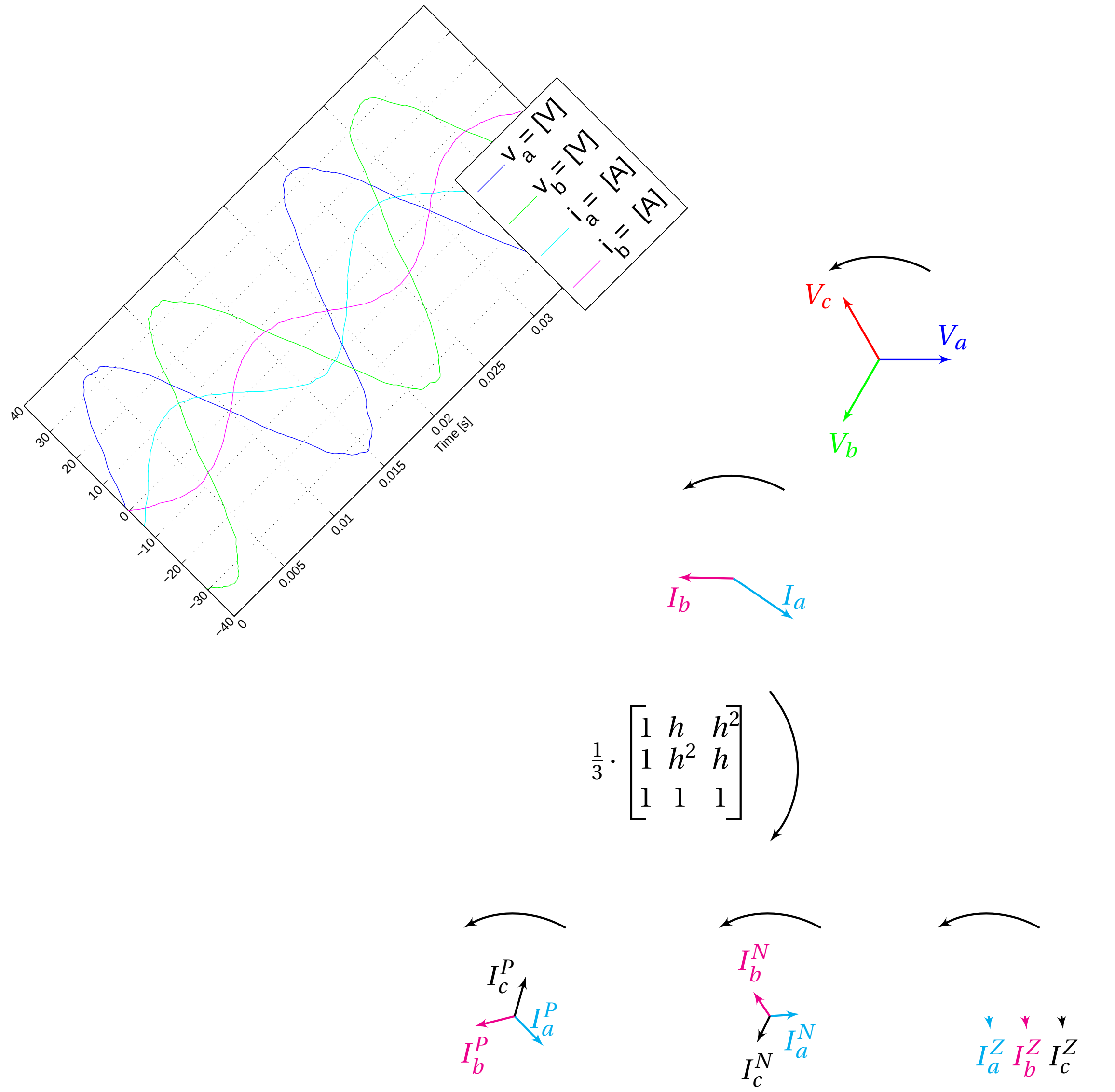

Master thesis in Electric Power Systems and High Voltage Engineering

Group: 2011 - EPSH4-1034
Board of Studies of Energy
Aalborg University

AALBORG UNIVERSITY

Title:	Synchronous and zero sequence impedance in a 60kV power system
Semester:	Master
Project period:	1/9, 2011 – 18/6, 2012
ECTS:	60
Supervisors:	Filipe Miguel Faria Da Silva Jan Møller (Nyfors A/S)
Project group:	EPSH4-1034

SYNOPSIS:

The aim of this thesis is to determine if the way the zero phase sequence impedance is calculated by Nyfors A/S today is accurate enough, and if not give new recommendation on how to obtain the positive- and zero phase sequence impedance. It is done by creating a model in PSCAD, which is validated by a set of measurements made on a 60kV cable owned by Nyfors A/S. The parameters of the model were tested in order to see which had influence on the zero phase sequence impedance and which have influence on the positive phase sequence impedance.
The guidelines at the end of the report are based on the model and the measurements.

Kenneth Rønsig Kanstrup

Copies:	4
Last page:	65
Last appendix:	B

By signing this document, each member of the group confirms that all participated in the project work and thereby all members are collectively liable for the content of the report.

Preface

The following report represents the master thesis titled "Synchronous and zero sequence impedance in a 60kVpower system" written by Kenneth Rønsig Kanstrup, group EPSH4-1034 at Department of Energy Technology at Aalborg University. The report was prepared during the period from the 1st September 2011 to 31st May 2012.

The report is organised in 12 chapters and subchapters which are identified by numbers. Figures, tables and equations are identified by their chapter number in A.B format, where A represents the chapter number and B the identification number. References are shown in the following format [X]. Finally, appendices identified by chapter letters are included after the bibliography.
The enclosed CD-ROM contains the written project in PDF format, MATLAB scripts for generation of plots from measurements and simulations, some of the references, models made in PSCAD and COMSOL Multiphysics. A list of the contends can be found in appendix B on page A3.

Unless otherwise is stated, voltages and currents are given by their RMS values. Voltages and currents in their phase values unless otherwise is specified.

I thank the Danish DSO Nyfors A/S for providing data on the cable which has been modelled and for help with the measurements.

Danish summary

Denne rapport omhandler måling og modellering af synkron- og nulimpedanser i et 60kV kabelanlæg ejet af elselskabet Nyfors A/S. Kablet er 18,708km langt og forbinder de to 60/10kV transformerstationer Agdrup (Brønderslev) og Jetsmark (Pandrup).

Det første der er beskrevet i rapporten er forskellige fejltyper, der kan opstå i et transmissionssystem. Fejlene er beskrevet med grundlæggende impedanser, hvor der er lagt vægt på hvilke typer af kortslutninger, der kan opstå i et kabelanlæg. Sekvens impedanser er også beskrevet for relevante fejltyper, hvor der er lagt vægt på udregning af fejlstrømme.

Kablet blev modelleret i PSCAD for at synliggøre om, der er en sammenhæng mellem synkron- og nulimpedans. Der blev foretaget målinger på kablet for at validere modellen. Udfra målingerne kunne det ses at modellen ikke var nøjagtig i alle tilfælde, hvilket ledte til en følsomhedsanalyse for at få optimeret modellen. Følsomhedsanalysen blev udført for både nulsekvens og for trefaset kortslutning til jord, dette gav at nogle af de testede værdier skulle justeres for at få en mere nøjagtig model.

Fra følsomhedsanalysen kunne det ses at nogle af værdierne havde en høj indflydelse på enten nulimpedansen eller på synkronimpedansen, dette blev antaget som den primære grund til, at den hidtidige metode for beregning af nulimpedans var unøjagtig.

Der er slutteligt i rapporten blevet udfærdiget et sæt retningslinier til bestemmelse af synkron- og nulimpedans.

Table of contents

1 Introduction

The Danish power grid is going through significant changes, from an Overhead Line (OHL) grid, towards an underground cable grid. This transformation is made due to Danish legislation on transmission systems, which states that all transmission lines with a voltage lower than 150kV must be converted to underground cables before 2039[1]. The main idea of these guidelines is, to meet a growing interest in keeping nature untouched by technical installations.

At the moment the Danish distribution system operator (DSO) Nyfors A/S, has 38km of 60kV cable. Due to the changes which have to be made to the Danish power system, this can become 150km in the future. Nyfors A/S is concerned that the types of faults in the power system will change with the change in the power system. The importance of getting the protection relays set correctly is evident. The concern is that double ground faults will be higher compared to two or three phased short-circuits.

The distance protection relays need the Positive Sequence (PPS) and Zero Sequence (ZPS) impedance in order to measure correctly for the double ground faults. This makes it important to know if the values for PPS impedance, and ZPS impedance are accurate enough. The consequences, of protection relays not being set correctly, can result in major inconveniences for the 44000 consumers, who are supplied from the Nyfors A/S grid. The result can either be that the distance protection does not disconnect fast enough, and therefore some of the equipment connected to the power system can be damaged, or the relays will disconnect on errors on other lines. In both cases the result could be frequent or major power failure.

The aim of this project is to write guidelines on how to calculate the impedance of 60kV cables. The impedance is needed in order to set the distance protection relays. The guidelines will help to check if the values, which are used today, are good enough, or if the impedances in all cable lines have to be measured in order to get optimal protection.

I PROBLEM ANALYSIS

2 Types of faults

This chapter will describe different types of faults, their characteristics and how they occur. In this chapter some assumptions will be made for easier comparison: the length from source to fault is the same in all cases, the line voltage is the same in all cases. Sequence components will not be taken into consideration since this is only made to compare the different types of faults. The sequence components will be described in chapter 3 on page 9 for the faults relevant to the Nyfors A/S power system.

2.1 One phase to ground

This type of fault is the most common of faults where one phase conductor comes into contact with the ground or earth conductor. This can happen if one cable is damaged due to digging or insulation faults in one cable, or if one conductor, in an OHL system, falls to the ground.
This gives the equation for the fault current which can be seen in equation 2.2.

$$Z = Z_{conductor} + Z_{ground} + Z_{fault} \qquad [\Omega] \quad (2.1)$$

$$I_{fault} = \frac{V_{phase}}{Z} \qquad [A] \quad (2.2)$$

A sketch of a one phase to ground fault in phase a, can be seen in figure 2.1.

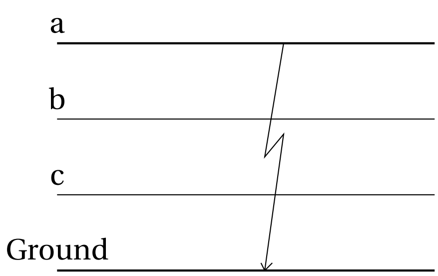

Figure 2.1: Sketch of one phase to ground short-circuit.

2.2 Two phase short-circuit

This type of fault occurs when two phase conductors come into contact with each other without touching ground, this type of fault is more common in an OHL system than in a cable system. The only way this can occur in a cable system is if the cable is a three phase cable with a united screen for all three conductors, which is mostly used as submarine cables.

Cables used in power systems in the ground are often one phase cables in which each conductor has separate screening and the screen is grounded so this short-circuit highly unlikely instead it will be a two phase to ground short-circuit which occurs.
The current for this type of fault can be calculated with equation 2.4.

$$Z = Z_{conductor} + Z_{conductor} + Z_{fault} = 2 \cdot Z_{conductor} + Z_{fault} \qquad [\Omega] \quad (2.3)$$

$$I_{fault} = \frac{V_{line}}{Z} \qquad [A] \quad (2.4)$$

A sketch of the two phase short-circuit can be seen in figure 2.2.

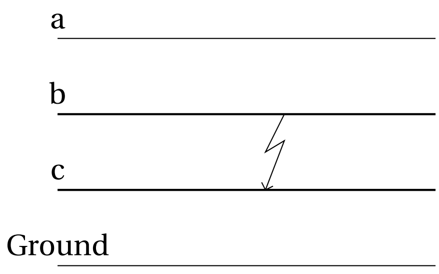

Figure 2.2: Sketch of two phase short-circuit.

2.3 Two phase to ground short-circuit

The two phase to ground fault will happen if there is a two phase short-circuit that comes into contact with a ground potential (ground, grounded conductor). This type of fault is more common than the two phase short-circuit in cable systems, since the cables are put into the ground, and each conductor is often shielded with a grounded shield. A sketch of this type of fault can be seen in figure 2.3.
The two phase to ground fault will have a higher current, than the two phase short-circuit since the ground will be in parallel to the conductors and therefore reduce the size of the total impedance as seen in equation 2.5.

$$Z = Z_{conductor} + Z_{fault} + \frac{1}{\frac{1}{Z_{conductor}} + \frac{1}{Z_{ground}}} \qquad [\Omega] \quad (2.5)$$

$$I_{fault} = \frac{V_{line}}{Z} \qquad [A] \quad (2.6)$$

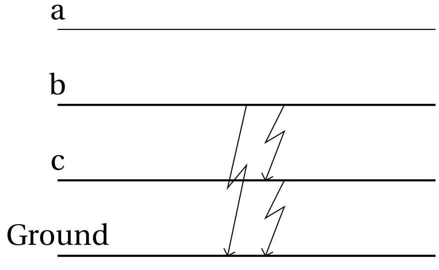

Figure 2.3: Sketch of two phase to ground short-circuit.

2.4 Double ground fault

This fault occurs if two conductors have a one phase to ground fault, without a short-circuit between the two phases. This can happen if two OHL fall to the ground without touching each other. In cable systems this can happen if two conductors have a ground fault without coming into contact with each other. The fault current can be calculated as two single phase short-circuits as seen in equation 2.1 and 2.2 on page 5 for each fault. This type of fault can be seen in figure 2.4.

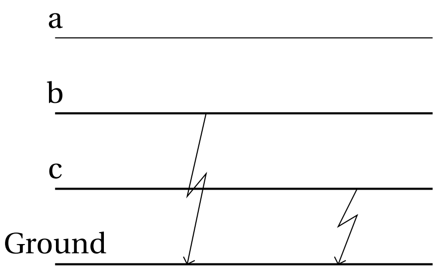

Figure 2.4: Sketch of two phase short-circuit.

2.5 Three phase short-circuit

The three phase short-circuit is a symmetrical fault, where the sum of the voltage in the three phases will always be equal to zero eg. $V_a + V_b + V_c = 0$. Consequently the sum of the currents also is zero eg. $I_a + I_b + I_c = 0$. Therefore, there is no return path for the current since it has been cancelled out by the current in the other phases. Therefore, the total impedance is as calculated in equation 2.7. It can be seen from equation 2.8 that this is the type of fault with the highest fault current.

$$Z = Z_{conductor} + Z_{fault} \quad [\Omega] \quad (2.7)$$

$$I_{fault} = \frac{V_{line}}{Z} \quad [A] \quad (2.8)$$

It can be seen from equation 2.7 that the impedance is the lowest of the impedances calculated in this chapter, and therefore the current must be the highest. This type of fault is sketched in figure 2.5.

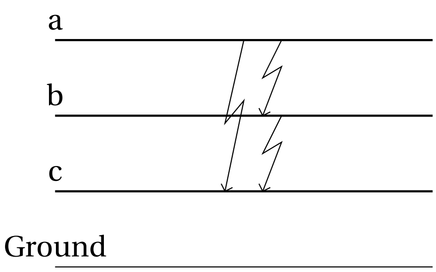

Figure 2.5: Sketch of three phase short-circuit.

Like the two phase short-circuit this fault is unlikely in a cabled power system since all phases have their own grounded screen, which will always come into contact with a short-circuit.

2.6 Three phase to ground short-circuit

This type of fault occurs if a three phase short-circuit comes into contact with the ground or a grounded conductor. The short-circuit can be calculated as three single phase short-circuits happening at the same location at the same time, if the fault is symmetrical the ground current will be equal to zero, due to the 120° phase angle existing in a symmetrical power system. The fault current can be calculated with equations 2.9 to 2.10.

$$Z = Z_{conductor} + Z_{fault} + Z_{ground} \qquad [\Omega] \quad (2.9)$$

$$I_a = \frac{V_a}{Z} \qquad [A]$$

$$I_b = \frac{V_b}{Z} \qquad [A]$$

$$I_c = \frac{V_c}{Z} \qquad [A]$$

$$I_{fault} = I_a + I_b + I_c \qquad [A] \quad (2.10)$$

If the fault is not symmetrical eg. $I_a + I_b + I_c \neq 0$, the ground current will be equal to $I_a + I_b + I_c$.

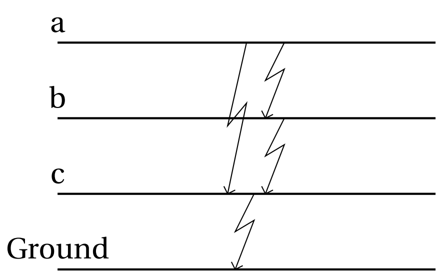

Figure 2.6: Sketch of unsymmetrical three phase short-circuit.

2.7 Conclusion

In this chapter different types of faults in a power system have been described and compared. The types of faults, which are likely to occur in the Nyfors A/S power system have been chosen for analysis with sequence components, the chosen faults are listed below.

- One phase to ground
- Two phase to ground
- Three phase to ground

The two phase clear of ground and three phase clear of ground will also be described even though these are highly unlikely.

3 Sequence components

This chapter will give a basic introduction to sequence components, and how to calculate the sequence currents of the different types of faults chosen in chapter 2.

3.1 Sequence components

The sequence components are used to calculate voltages and currents in unbalanced transmission system faults more easily. The sequence components divide the actual voltages and currents into a positive phase sequence (PPS), meaning that the phases are distributed with 120° phase lag between each phase and all three phases are equal in magnitude. A negative phase sequence (NPS), meaning that the phases are distributed with a 120° phase lead between each phase and all three phases are equal in magnitude. And a zero sequence in which the phases do not have any phase lag between them, but all three phases are still equal in magnitude. A graphical representation of the sequence components can be seen in figure 3.1.[2]

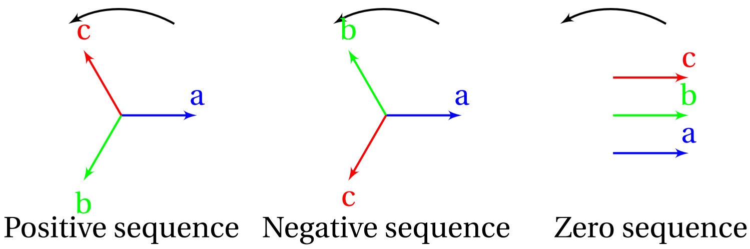

Figure 3.1: Graphical interpretation of sequence components.

The main part of transforming from sequence reference frame to phase reference frame is the **H** matrix which can be seen in equation 3.1, [2, 3].

$$\mathbf{H} = \begin{bmatrix} 1 & 1 & 1 \\ h^2 & h & 1 \\ h & h^2 & 1 \end{bmatrix} \tag{3.1}$$

In which:
h is the complex factor $1\angle 120°$
The notation of the **H** matrix is $\begin{bmatrix} \text{PPS} & \text{NPS} & \text{ZPS} \end{bmatrix}^T$, an example of how to use the **H** matrix can be seen in equation 3.2.

$$\begin{bmatrix} V_a \\ V_b \\ V_c \end{bmatrix} = \begin{bmatrix} 1 & 1 & 1 \\ h^2 & h & 1 \\ h & h^2 & 1 \end{bmatrix} \begin{bmatrix} V^P \\ V^N \\ V^Z \end{bmatrix} = \begin{bmatrix} V^P + V^N + V^Z \\ V^P \cdot h^2 + V^N \cdot h + V^Z \\ V^P \cdot h + V^N \cdot h^2 + V^Z \end{bmatrix} \tag{3.2}$$

In order to calculate from phase reference frame to sequence reference frame the $\mathbf{H^{-1}}$ is needed. This matrix can be seen in equation 3.3.

$$\mathbf{H^{-1}} = \frac{1}{3} \cdot \begin{bmatrix} 1 & h & h^2 \\ 1 & h^2 & h \\ 1 & 1 & 1 \end{bmatrix} \tag{3.3}$$

3.2 One phase to ground

For the calculation of the currents in this type of fault the load currents are neglected, so that the current of the non-affected phases is zero as shown in equation 3.4. This example is for a fault occurring in phase a as seen in the sketch of the fault in figure 2.1 on page 5.

$$\mathbf{I^{PNZ}} = \mathbf{H^{-1}} \cdot \mathbf{I_F} \qquad [A]$$

$$\begin{bmatrix} I^P \\ I^N \\ I^Z \end{bmatrix} = \frac{1}{3} \cdot \begin{bmatrix} 1 & h & h^2 \\ 1 & h^2 & h \\ 1 & 1 & 1 \end{bmatrix} \begin{bmatrix} I_a \\ 0 \\ 0 \end{bmatrix} = \frac{1}{3} \cdot \begin{bmatrix} I_a \\ I_a \\ I_a \end{bmatrix} \qquad [A] \tag{3.4}$$

As it can be seen from equation 3.4 the current of the sequence components is the same for all components which means that the PPS, NPS and ZPS impedances must be in series. A diagram of the one phase fault in sequence networks can be seen in figure 3.2.

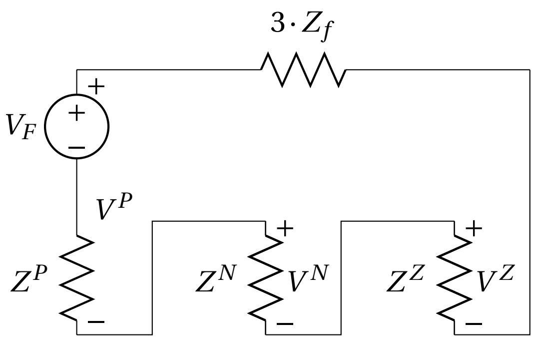

Figure 3.2: Impedances of the sequence network for a one phase to ground fault [3].

Where:
V_F is the voltage of phase a.

The fault voltage can be stated as:

$$V_F = \begin{bmatrix} Z^P + Z_F & Z^N + Z_F & Z^Z + Z_F \end{bmatrix} \begin{bmatrix} I^P \\ I^N \\ I^Z \end{bmatrix} \qquad [V] \tag{3.5}$$

By knowing the fault voltage, from equation 3.5 and that the currents are equal to each other $I^P = I^N = I^Z$, from equation 3.4, the sequence current can be calculated as stated in equation 3.6.

$$I^P = \frac{V_F}{Z^P + Z^N + Z^Z + 3 \cdot Z_F} \qquad \text{[A]} \quad (3.6)$$

3.3 Two phase to ground faults

For the first part of this section the fault will be a double ground fault as described in section 2.4 on page 7 since these calculations are basicly the same as for the two phase to ground short-circuit[3]. The first fault will be a ground fault in phase b and phase c. The second fault will be a short-circuit between phase b, phase c and ground, in both cases the load current will be neglected and therefore $I_a = 0$. An equivalent diagram of the fault in sequence reference frame can be seen in figure 3.3.

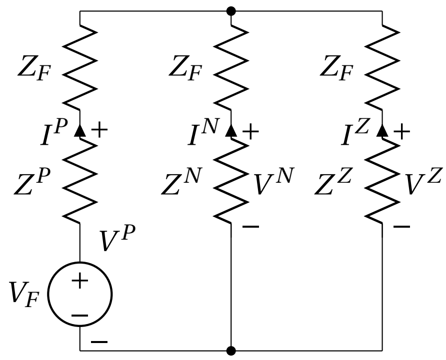

Figure 3.3: Impedances of the sequence network for a two phase to ground short-circuit [3].

From figure 3.3 Kirchoff's current equation can be determined to be:

$$I^P + I^N + I^Z = 0 \qquad \text{[A]} \quad (3.7)$$

$$\Updownarrow$$

$$I^Z = -\left(I^P + I^N\right) \qquad \text{[A]} \quad (3.8)$$

V_b and V_c can be determined from equation 3.2 on page 9, equation 3.9 to 3.11 is needed for obtaining the sequence voltages, when the voltages of phase b and c are of opposite polarity.

$$V_b - V_c = \left(V^P \cdot h^2 + V^N \cdot h + V^Z\right) - \left(V^P \cdot h + V^N \cdot h^2 + V^Z\right) \qquad \text{[V]} \quad (3.9)$$

$$\Updownarrow$$

$$V_b - V_c = \left(h^2 - h\right) \cdot V^P + \left(h - h^2\right) \cdot V^N = Z_F \cdot \left[\left(h^2 - h\right) \cdot I^P + \left(h - h^2\right) \cdot I^N\right] \qquad \text{[V]} \quad (3.10)$$

$$\Downarrow$$

$$V^P - Z_F \cdot I^P = V^N - Z_F \cdot I^N \qquad \text{[V]} \quad (3.11)$$

Equations 3.12 to 3.14 are used in order to obtain the sequence voltages when the voltages of phase b and c are of the same polarity.

$$V_b + V_c = \left(V^P \cdot h^2 + V^N \cdot h + V^Z\right) + \left(V^P \cdot h + V^N \cdot h^2 + V^Z\right) \quad [V] \quad (3.12)$$

$$\Updownarrow$$

$$\begin{aligned} V_b + V_c &= \left(h^2 + h\right) \cdot V^P + \left(h + h^2\right) \cdot V^N + 2 \cdot V^Z \\ &= Z_F \cdot \left[\left(h^2 + h\right) \cdot I^P + \left(h + h^2\right) \cdot I^N + 2 \cdot I^Z\right] \end{aligned} \quad [V] \quad (3.13)$$

$$\Downarrow$$

$$2 \cdot V^Z - 2 \cdot Z_F \cdot I^Z = V^P - Z_F \cdot I^P + V^N - Z_F \cdot I^N \quad [V] \quad (3.14)$$

By using equation 3.11, equation 3.14 can be rewritten as equation 3.16.

$$2 \cdot V^Z - 2 \cdot Z_F \cdot I^Z = 2 \cdot V^N - 2 \cdot Z_F \cdot I^N \quad [V] \quad (3.15)$$

$$\Downarrow$$

$$V^Z - Z_F \cdot I^Z = V^N - Z_F \cdot I^N = V^P - Z_F \cdot I^P \quad [V] \quad (3.16)$$

From the definitions $V^P = V_F - Z^P \cdot I^P$, $V_N = -Z^N \cdot I^N$ and $V_Z = -Z^Z \cdot I^Z$, which can be obtained from figure 3.3, the voltage equation 3.16 can be expressed by current and impedance in equation 3.17.

$$V_F - \left(Z^P + Z_F\right) \cdot I^P = -\left(Z^N + Z_F\right) \cdot I^N = -\left(Z^Z + Z_F\right) \cdot I^Z \quad [V] \quad (3.17)$$

From figure 3.3, Kirchoff's current law in equation 3.7 and equation 3.17 it can be seen, that the NPS and ZPS currents can be expressed by the use of I^P, as seen in equation 3.18 and reduced to an expression for I^P in equation 3.19.

$$I^P + \frac{\left(Z^P + Z_F\right) \cdot I^P - V_F}{\left(Z^N + Z_F\right)} + \frac{\left(Z^P + Z_F\right) \cdot I^P - V_F}{\left(Z^Z + Z_F\right)} = 0 \quad [A] \quad (3.18)$$

$$\Updownarrow$$

$$I^P = \frac{\left(Z^N + Z^Z + 2 \cdot Z_F\right) \cdot V_F}{3 \cdot Z_F^2 + 2 \cdot Z^P \cdot Z_F + 2 \cdot Z^N \cdot Z^F + 2 \cdot Z^Z \cdot Z_F + Z^P \cdot Z^N + Z^P \cdot Z^Z + Z^N \cdot Z^Z} \quad [A] \quad (3.19)$$

By doing the same as in equation 3.18 and 3.19 for I^N and I^Z, equation 3.20 and 3.21 can be obtained.

$$I^N = \frac{-\left(Z^Z + Z_F\right) \cdot V_F}{3 \cdot Z_F^2 + 2 \cdot Z^P \cdot Z_F + 2 \cdot Z^N \cdot Z^F + 2 \cdot Z^Z \cdot Z_F + Z^P \cdot Z^N + Z^P \cdot Z^Z + Z^N \cdot Z^Z} \quad [A] \quad (3.20)$$

$$I^Z = \frac{-\left(Z^N + Z_F\right) \cdot V_F}{3 \cdot Z_F^2 + 2 \cdot Z^P \cdot Z_F + 2 \cdot Z^N \cdot Z^F + 2 \cdot Z^Z \cdot Z_F + Z^P \cdot Z^N + Z^P \cdot Z^Z + Z^N \cdot Z^Z} \quad [A] \quad (3.21)$$

The current which goes to ground,I_E, is the sum of the current in phase b and phase c, this can be calculated as three times I^Z [3] as stated in equation 3.22.

$$3 \cdot I^Z = \frac{-3 \cdot \left(Z^N + Z_F\right) \cdot V_F}{3 \cdot Z_F^2 + 2 \cdot Z^P \cdot Z_F + 2 \cdot Z^N \cdot Z^F + 2 \cdot Z^Z \cdot Z_F + Z^P \cdot Z^N + Z^P \cdot Z^Z + Z^N \cdot Z^Z} \quad [A] \quad (3.22)$$

3.4 Three phase to ground short-circuit

In this section the power system is assumed balanced and therefore the current can be described as in equation 3.23 and the voltage can be described as in equation 3.24 to 3.26

$$I_a + I_b + I_c = 0 \quad [A] \quad (3.23)$$
$$V_a = Z^F \cdot I_a \quad [V] \quad (3.24)$$
$$V_b = Z^F \cdot I_b \quad [V] \quad (3.25)$$
$$V_c = Z^F \cdot I_a \quad [V] \quad (3.26)$$

From equation 3.23 the sequence currents can be determined with the help of equation 3.3.

$$\begin{bmatrix} I^P \\ I^N \\ I^Z \end{bmatrix} = \frac{1}{3} \cdot \begin{bmatrix} 1 & h & h^2 \\ 1 & h^2 & h \\ 1 & 1 & 1 \end{bmatrix} \begin{bmatrix} I_a \\ I_b \\ I_c \end{bmatrix} = \begin{bmatrix} 1 \\ 0 \\ 0 \end{bmatrix} \quad (3.27)$$

Equation 3.27 shows that the three phase short-circuit only consists of PPS currents. From this the equivalent diagram for this type of fault can be seen in figure 3.4. In this type of fault, the fault impedance Z_F for each phase is between phase and ground.This gives a sequence equivalent diagram as seen in figure 3.4.

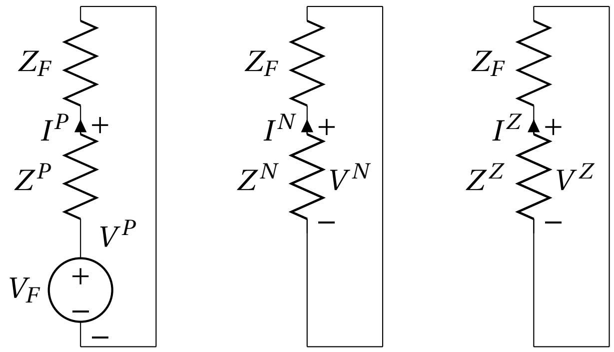

Figure 3.4: Impedances of the sequence network for a 3 phase short-circuit to ground [3].

From figure 3.4 equation 3.29 for the positive sequence current can be obtained, it can be seen that there is no voltage source in the NPS and the ZPS network and therefore the NPS and ZPS voltage must be 0, the PPS voltage can be determined as seen in equation 3.28.

$$V^P = Z_F \cdot I^P = V_F - Z^P \cdot I^P \quad [V] \quad (3.28)$$

From equation 3.28 I^P can be determined as in equation 3.29.

$$I^P = \frac{V_F}{Z_F + Z^P} \quad [A] \quad (3.29)$$

From this it can be seen that a three phase to ground short-circuit can be used to measure the PPS impedance.

4 System description

The system this project looks into is a 60kV cable line in the Nyfors A/S grid in the northern part of Jutland. The cable line connects the two 60kV substations in Jetsmark (JMK) and Agdrup (AGD), a map of the line can be seen in figure 4.1.

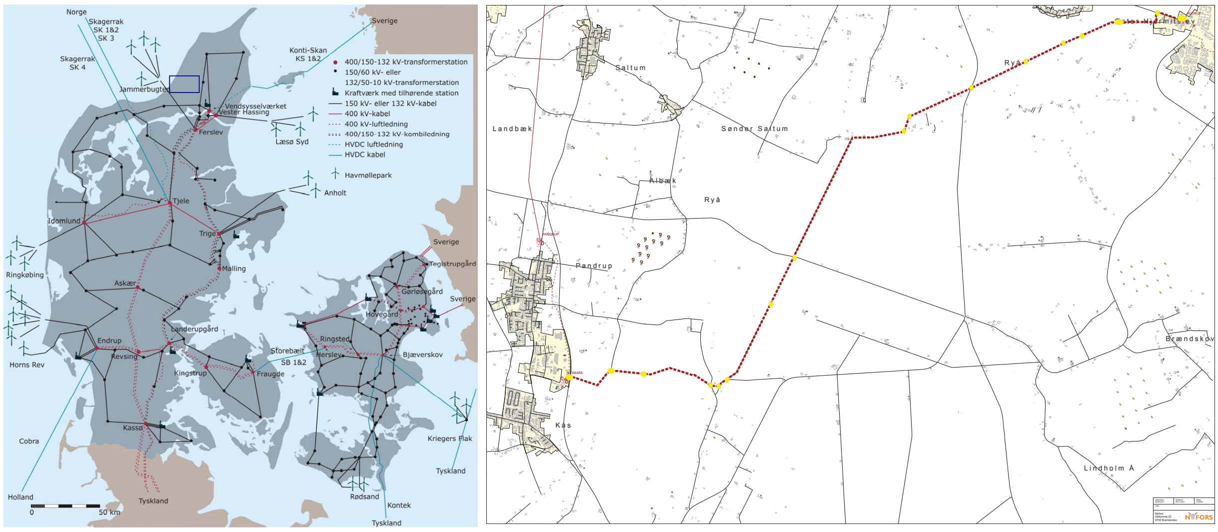

Figure 4.1: The location of the AGD-JMK cable line, is the thick red line, yellow areas are where the cable have been drilled under a creek or a road.

The cable is 18.708km long, and consists of three single core cables. The cables are laid in a trefoil formation in the entire length of the cable except 6m in AGD and 4m in JMK. The cables have no cross bonding and the connections are made so that the trefoil formation is preserved. The 10m of cable have no data on, how they are laid, and are a very little part of the cable (10m vs 18698m), and therefore the difference in the cable laying formation has been neglected in the model, and the cable is looked upon as laid in trefoil formation in the whole length of the cable, the cable formation can be seen in figure 4.2. The cable is laid in 1.3m debt in the entire length, in figure 4.1 there are areas marked with yellow. These are areas, where the cable has been drilled under a small river or a road, at these locations the cable is laid in an average of 2.8m, the total length of the under drilling is 696m. This have been calculated in Excel, the calculation can be found on the cd in: E:\Nyfors AS\Underdrillings\Dybder.xlsx.

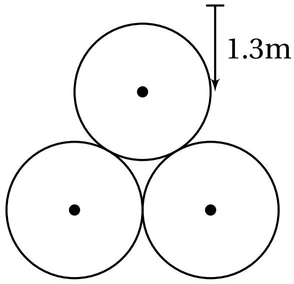

Figure 4.2: Cables are laid in trefoil formation.

4.1 Cable construction

The cables consist of an aluminum core with a cross section of 400mm^2. The inner insulation consists of Cross-linked polyethylene (XLPE). The metallic screen is consists of 60 copper wires with a diameter of 1.04mm, and an aluminum tape with a thickness of 0.13mm, the combined cross section of the metallic screen is 70mm^2. Between the insulation and the conducting layers (the core and the screen) there is a semi-conducting layer in order to ensure an even distribution of the electric field[4], the thickness of the semi-conducting layer is 0.8mm between the main conductor and the insulation and 0.6mm between the conducting screen and the insulation. The layers in the cable can be seen in figure 4.3.

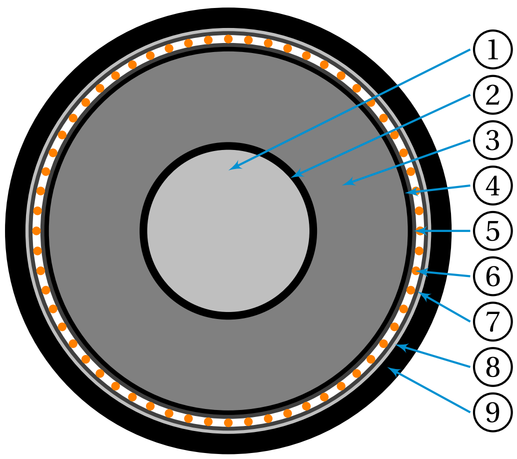

	Item
1	Conductor
2	Conductor screen
3	Insulation
4	Insulation screen
5	Water proof tape
6	Metallic screen
7	Water proof tape
8	Metallic screen
9	Outer sheath

Figure 4.3: Construction of cable, numbers are described in the table.

The different layers of the cable are described in table 4.1, the table contains a number for reference to figure 4.3, a description of what the layer is doing in the cable and what material the layer is made from and finally the outer radius of the layer, which has been calculated from the thickness of the layers in the cable.

	Item	Material	Outer radius
1	Conductor	aluminum, solid class1, IEC 60228	10.80mm
2	Conductor screen	Extruded semi-conducting layer	11.60mm
3	Insulation	Extruded dry cured XLPE	23.60mm
4	Insulation screen	Extruded semi-conducting layer	24.20mm
5	Water proof tape	Swellable semi-conducting tape	24.72mm
6	Metallic screen	Annealed copper wires	25.76mm
7	Water proof tape	Swellable semi-conducting tape	26.28mm
8	Metallic screen	aluminum/copolymer tape	26.40mm
9	Outer sheath	Extruded MDPE	29.40mm

Table 4.1: Data sheet handed out by Nyfors A/S.

The data sheet for the cable, handed out by Nyfors A/S, can be seen in table A.1 in appendix A.

5 Problem statement

As described in the previous chapters the sequence components are an important part of the setting of distance protection. Today the calculation of ZPS impedance of cables is done from guidelines intended for OHL[5]. This project will give recommendations on how to obtain the PPS and ZPS impedance before setting the distance protection.

This gives a main problem of this project:

Is the guidelines for obtaining the PPS and ZPS impedance, which is used today. accurate enough.

5.1 Method

The sequence impedances of the line from AGD to JMK will be determined from measurements in the field and a PSCAD model.

The magnetic field in the cable system will be investigated with a finite element model made in COMSOL Multiphysics.

The new guidelines for obtaining the sequence components will be written, based on the model of the AGD to JMK cable.
To verify the model the simulation results will be compared with the measurements of the AGD to JMK cable line.

5.2 Limitations

The 10m cable which are not laid in trefoil will not be considered.

II PROBLEM SOLVING

6 PSCAD modeling

The purpose of the PSCAD model is to make a basis for the new guidelines for future calculation of the PPS and ZPS impedance. The model will be validated with values obtained by field measurements in chapter 7, the test set-up used for the field measurements is described in section 6.2.

6.1 Modelling cable in PSCAD

In order to model a cable in PSCAD the first parameter and easiest parameter to determine is the depth and horizontal location of the three cables.

6.1.1 Depth of cable

According to Nyfors A/S the depth of the cables 1.3m, as seen in figure 4.2 on page 16, which is assumed to be the depth of the centre of the top conductor of the trefoil formation. The diameter of the cables is 58.8mm, this gives a horizontal distance of the centre of the two bottom cables to be 58.8mm and therefore the horizontal distance to the centre of each cable from the centre of the top cable is 29.4mm. The depth of the two bottom cables can be calculated by using equation 6.1.

$$l_{2,3_{depth}} = l_{1_{depth}} + \sqrt{(2\cdot r)^2 - r^2} = 1.3 + \sqrt{(2\cdot 0.0294)^2 - 0.0294^2} = 1.3509 \qquad \text{[m]} \quad (6.1)$$

The depth of the underdrillings is calculated, by taking the average of all measurements, in the drilling reports (found on the CD) deeper than 130cm. The average depth has been calculated be to 280cm in chapter 4.

6.1.2 Inner conductor

The conductive layers of the cable needs three parameters: inner radius, outer radius and resistivity. The way to model a solid conductor in PSCAD is to set the inner radius to 0mm. The outer diameter is given in the data-sheet to be 21.6mm, which gives a radius of 10.3mm. The resistivity can be set to $2.8\cdot 10^{-8}$, which is the resistivity of aluminum.

6.1.3 Inner insulator

The insulator needs two parameters: the outer radius and the permittivity. The outer radius is calculated by summing the radius of the inner conductor and the thickness of the insulating layers; the conductor screen, insulation, insulation screen and the inner waterproof tape. This is summed up to be 24.72mm, as seen in table 4.1 on page 17. The relative permittivity is set to be 2.3 for the insulation layer, the permittivity of the semiconducting layers is much higher and can therefore be neglected[6]. On the other hand the thickness of the semiconducting layers cannot be neglected and the permittivity of the insulating layer are therefore corrected. The capacitance of the cable is calculated by means of equation 6.2.

$$C = \epsilon \cdot \frac{2 \cdot \pi \cdot l}{ln\,(b/a)} \qquad [F] \quad (6.2)$$

For the correction factor of the permittivity ϵ', the capacitance and length of the cable is held constant, the calculation of ϵ' is done in equation 6.3.

$$\epsilon' = \epsilon \cdot \frac{ln\,(r_2/r_1)}{ln\,(b/a)} \qquad [-] \quad (6.3)$$

Where:
a and b are the inner and outer radius of the insulation.
r_1 and r_2 are the outer radius of the conductor and the inner radius of the metallic screen.

This gives a corrected permittivity of which is calculated in equation 6.4.

$$\epsilon' = 2.3 \cdot \frac{ln\,(24.72/10.8)}{ln\,(23.6/11.6)} = 2.68 \qquad [-] \quad (6.4)$$

6.1.4 Metallic screen

As the inner conductor the metallic screen needs two parameters: outer radius and resistivity. The outer radius can be found in table 4.1 on page 17 and is stated here for revision purposes 24.4008mm. An equivalent of the resistivity has to be calculated since the screen consists of copper strands and aluminum tape. The layers are connected at the ends and can therefore be looked upon as one layer. The first thing in order to calculate the resistivity of the screen, is to calculate the resistance of the copper part. This calculation is done in equation 6.5[7]. The nominal area and the thickness of the copper strands can be found in the data-sheet in table A.1 on page A1.

$$\rho'_{cu} = \rho_{cu} \cdot \frac{\left(r_{out}^2 - r_{in}^2\right) \cdot \pi}{A} \qquad [\Omega \cdot \mathrm{m}]$$

$$\rho'_{cu} = 1.724 \cdot 10^{-8} \cdot \frac{\left(25.76^2 - 24.72^2\right) \cdot \pi}{50} = 5.6868 \cdot 10^{-8} \qquad [\Omega \cdot \mathrm{m}] \quad (6.5)$$

The next step is to find the area of the aluminum tape, which is the difference between the total area of the screen and the area of the copper part of the screen, which are both is given in the data-sheet handed out by Nyfors A/S. Here it is stated that the aluminum tape is 20mm^2. The equivalent resistivity is calculated by means of equation 6.6[7].

$$\rho_{eq} = \rho'_{cu} \cdot \frac{A_{cu}}{A_{al} + A_{cu}} + \rho_{al} \cdot \frac{A_{al}}{A_{al} + A_{cu}} \qquad [\Omega \cdot \mathrm{m}]$$

$$\rho_{eq} = 5.6868 \cdot 10^{-8} \cdot \frac{50}{70} + 2.8 \cdot 10^{-8} \cdot \frac{20}{70} = 4.8706 \cdot 10^{-8} \qquad [\Omega \cdot \mathrm{m}] \quad (6.6)$$

6.1.5 Overview of PSCAD cable model

In figure 6.1 the cable editor in PSCAD can be seen.

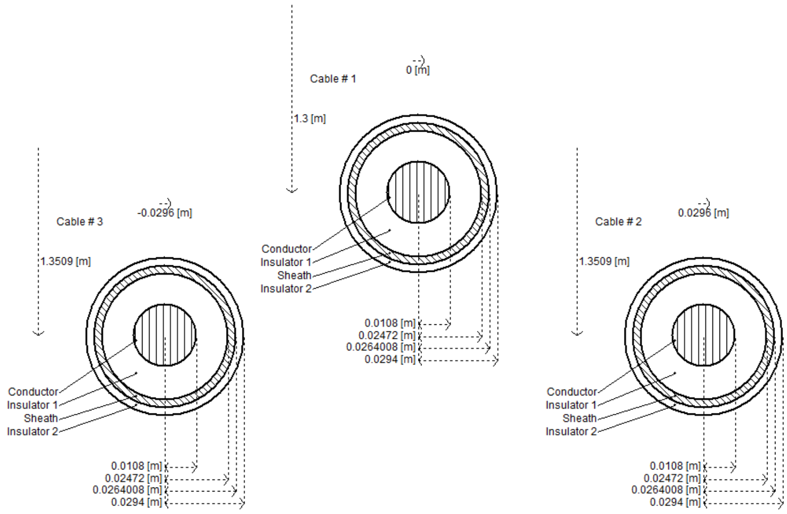

Figure 6.1: Overview of the cable editor in PSCAD.

6.2 Test set-up

In order to create test set-ups, the tests have to be chosen. Since the model is to be used to determine sequence components of short-circuits in the cable, the tests have to deal with the possible short-circuits in the system. In order to find the PPS/NPS impedance it is necessary to make a three phase short-circuit to ground, since this consists of only PPS components as described in section 3.4 on page 13. The ZPS impedance can be measured by adding the same phase to all three conductors and short-circuit the three conductors to ground at the other end[3].
These tests will give some impedance values from which the model can be generated. in order to have some values from which the model can be validated, more tests have to be made.

It has been chosen to make tests of single phase to ground and two phase to ground faults since these contain both PPS, NPS and ZPS impedances. This gives a possibility to validate the model form faults which contain all sequence components.

When doing the tests the remaining phases will be connected during the test in order to simulate the system in operation where all phases will be energized if a fault should occur. This is done because the energization of the other cables, has an influence on the impedance of the cable, which is being tested. The terminal numbers are not available, since the connection will be done at cable ends in the high voltage system.

The tests have been simulated in section 6.3. A sketch of the test set-ups can be seen in the sections for the simulation of the respective tests. The results of the simulations can be seen in table 6.1 in section 6.4 on page 35.

The measurements will be taken at JMK where the test equipment will be connected directly at the cable ends. At the AGD end the short-circuits will be made by Nyfors A/S with equipment owned by Nyfors A/S.

6.2.1 Test set-up in PSCAD

The test set-up have been simulated in PSCAD, the modelling of the system can be seen in figure 6.2.

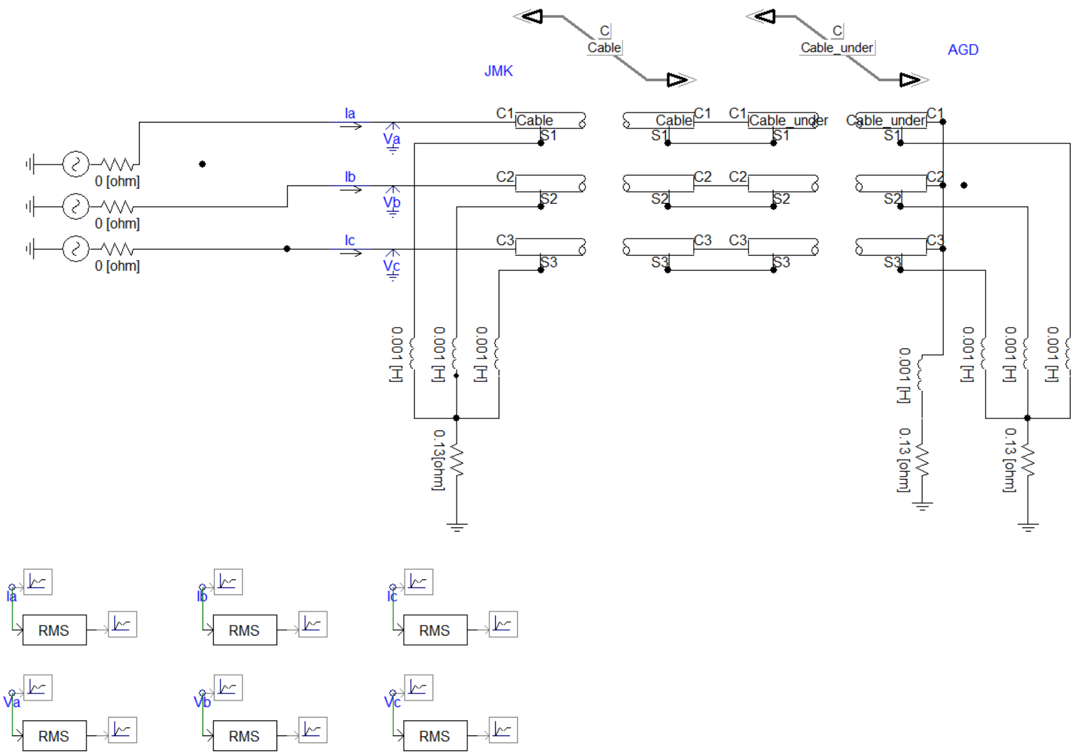

Figure 6.2: Overview of the test set-up, for three phase to ground test, modelled in PSCAD.

In the set-up three single phase voltage generators are used for supplying the cable, as it can be seen in table 7.1 on page 37. In the field measurements this is done by a three phase auto transformer. The cable has been divided into two sections one at a depth of 1.3m and one in which the depth have been set to 2.8m, which is the average depth of the underdrillings. The ground impedance has been divided into an inductive part and a resistive part, the inductive part has been set to 1mH and the resistive part has been set to 0.13Ω.

6.3 Test simulation results

This section will contain figures of test set-ups, simulation results from the PSCAD model of the different short-circuit tests. The figures and data of the simulation results are available on the CD in: E:\Simulation models\PSCAD\Original model\Simulation results*. The model will be compared to the measurement results in section 7.2 on page 41.

6.3.1 One phase to ground short-circuit

The test set-up for the one phase fault can be seen in figure 6.3. The sketch is made for phase a and the other tests have the same set-up except for the short-circuit to ground which will be moved to phase b and c respectively.

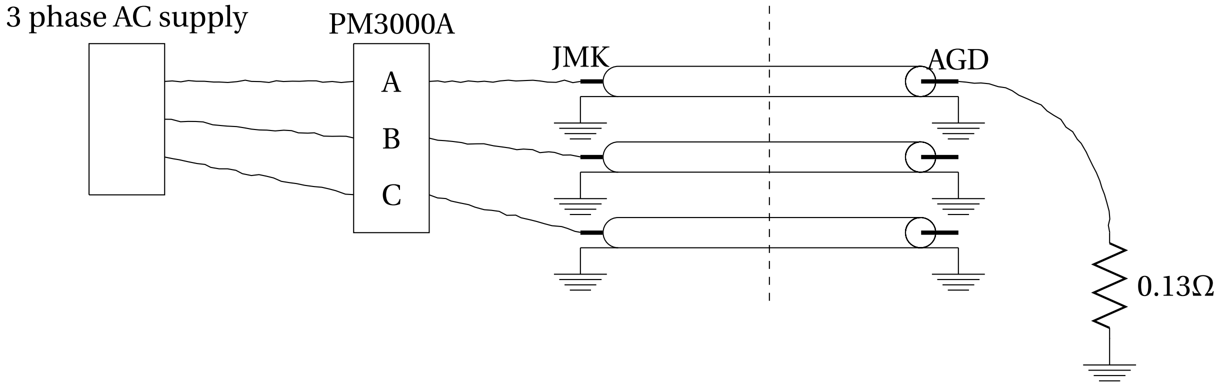

Figure 6.3: Test set-up of one phase to ground fault in phase a.

The simulation results of the one phase short-circuit can be seen in figures 6.4 to 6.9. In all cases the load has been disconnected and therefore the only phase of interest, is the one, in which the short-circuit appears.

Phase a to ground

Figure 6.4 shows the result of a short-circuit in phase a, figure 6.5 shows a zoom of the steady state result of the simulation. The RMS voltage has been set to 23.06V, and the RMS current is calculated to $5.56\angle -41.4$A in phase a.

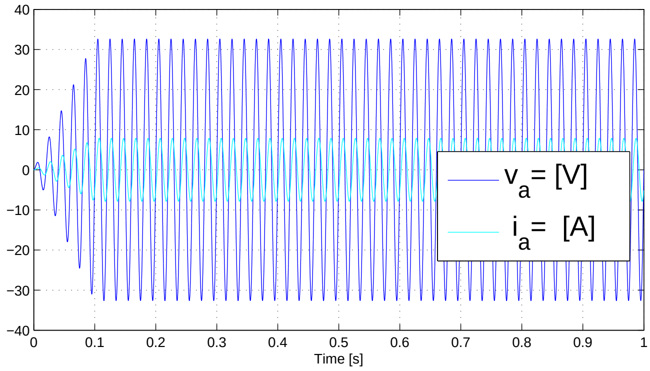

Figure 6.4: Result of simulation of one phase to ground short-circuit in phase a.

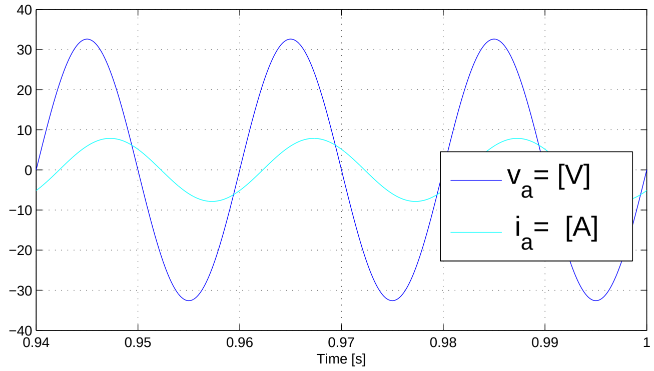

Figure 6.5: Zoom view of the result of simulation of one phase to ground short-circuit in phase a.

Phase b to ground

Figure 6.6 shows the result of a short-circuit in phase b, figure 6.7 shows a zoom of the steady state result of the simulation. The RMS voltage has been set to 22.67V, and the RMS current is calculated to $5.46\angle -39.6$A in phase b.

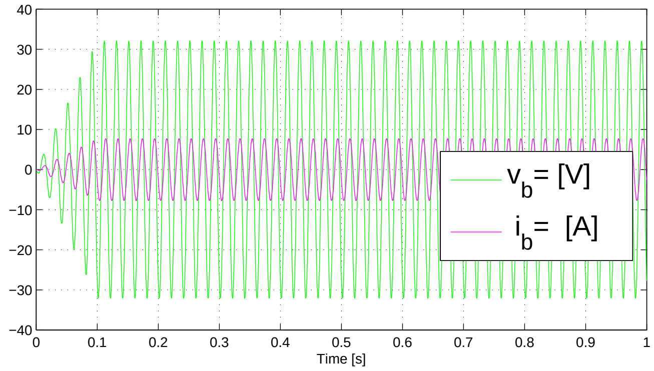

Figure 6.6: Result of simulation of one phase to ground short-circuit in phase b.

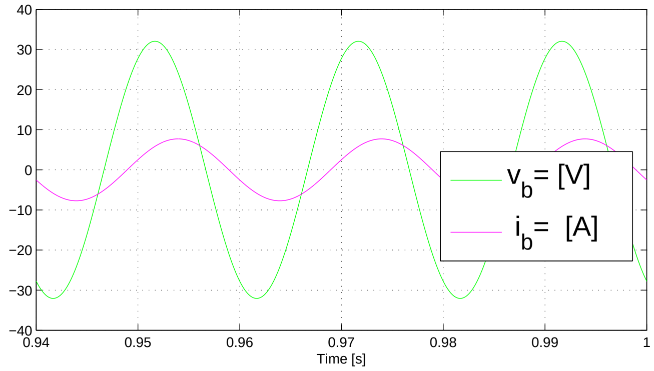

Figure 6.7: Zoom view of the result of simulation of one phase to ground short-circuit in phase b.

Phase c to ground

Figure 6.8 shows the result of a short-circuit in phase c, figure 6.9 shows a zoom of the steady state result of the simulation. The RMS voltage has been set to 22.44V, and the RMS current is calculated to $5.41\angle -41.4$A in phase c.

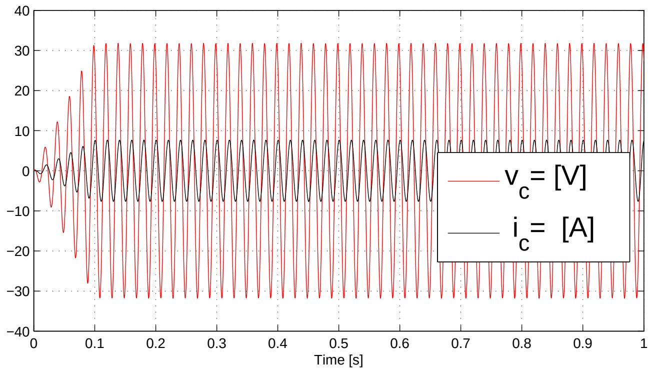

Figure 6.8: Result of simulation of one phase to ground short-circuit in phase c.

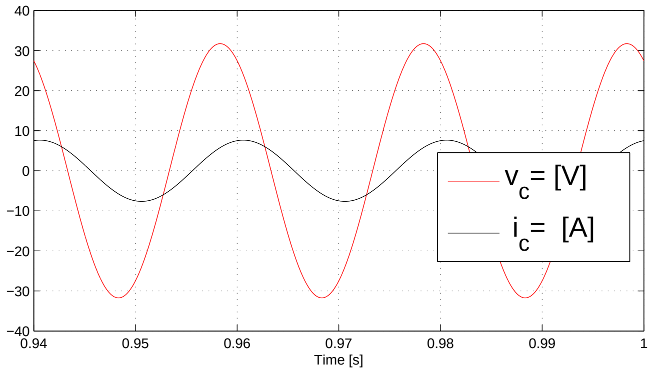

Figure 6.9: Zoom view of the result of simulation of one phase to ground short-circuit in phase c.

6.3.2 Two phase to ground short-circuits

This test set-up is for the two phase to ground short-circuit and can be seen in figure 6.10, the same test set-up is used for all two phase short-circuit tests, also when the short-circuit is moved to the other phases.

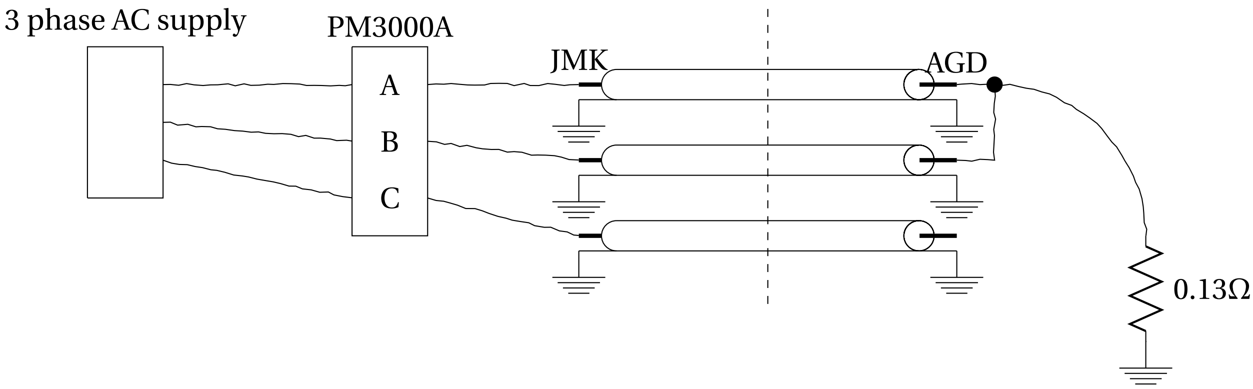

Figure 6.10: Test set-up of two phase short-circuit to ground fault in phase a and b.

The results of the two phase short-circuit to ground can be seen in figures 6.11 to 6.16.

Phase a and b to ground

The result of the short-circuit between phase a and b can be seen in figure 6.11, a zoom view of the steady state result can be seen in figure 6.12. The RMS values for the phase voltage have been set to V_a = 22.84V and V_b = 23.97V and current has been calculated to be $I_a = 7.81\angle -37.8$A and $I_b = 6.71\angle -63.0$A.

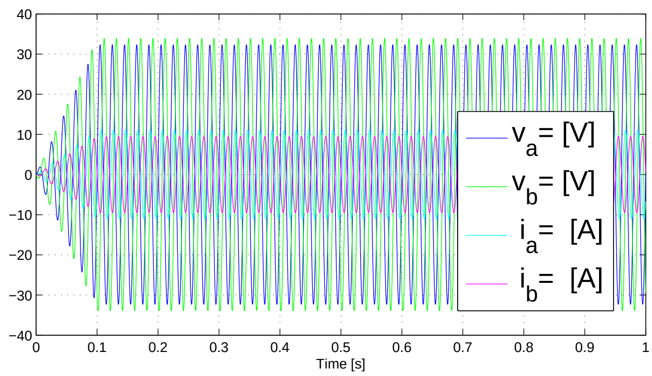

Figure 6.11: Result of simulation of two phase to ground short-circuit in phase a and b.

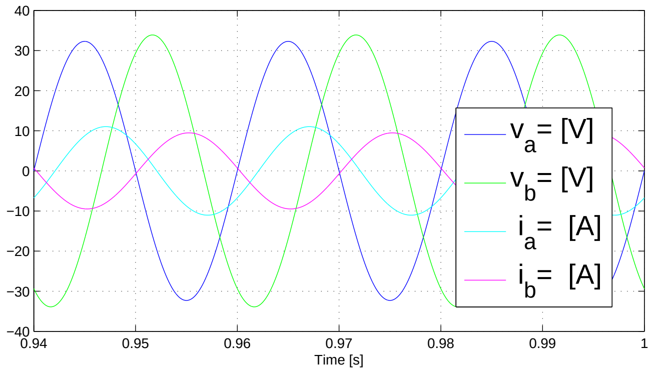

Figure 6.12: Zoom view of the result of simulation of two phase to ground short-circuit in phase a and b.

Phase a and c to ground

The result of the short-circuit can be seen in figure 6.13, a zoom view of the steady state result can be seen in figure 6.14. The RMS values for the phase voltage have been set to $V_a = 23.04$V and $V_c = 22.21$V and current has been calculated to be $I_a = 6.46\angle-64.8$A and $I_c = 7.56\angle-37.8$A

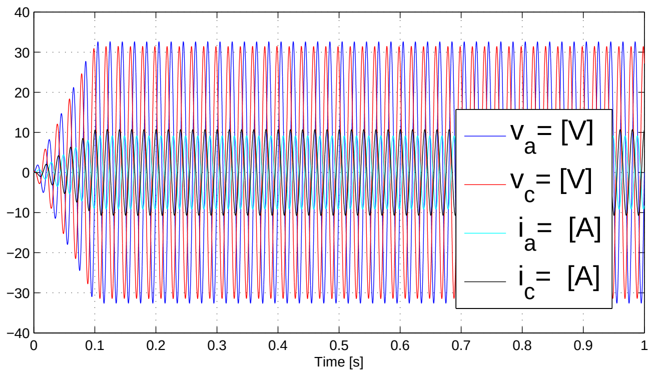

Figure 6.13: Result of simulation of two phase to ground short-circuit in phase a and c.

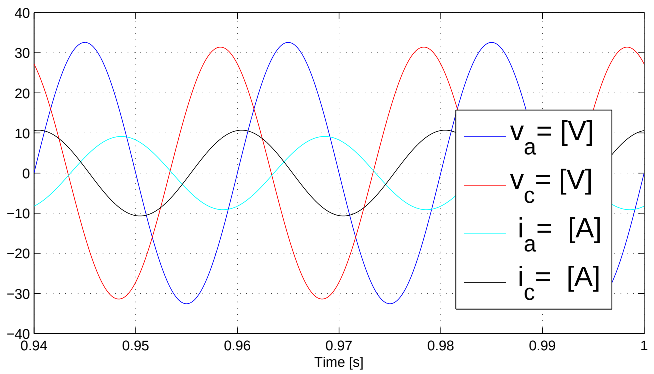

Figure 6.14: Zoom view of the result of simulation of two phase to ground short-circuit in phase a and c.

Phase b and c to ground

The result of the short-circuit can be seen in figure 6.15, a zoom view of the steady state result can be seen in figure 6.16. The RMS values for the phase voltage have been set to $V_b = 23.36$V and $V_c = 24.39$V and current has been calculated to be $I_b = 7.96\angle -37.8$A and $I_c = 6.82\angle -64.8$A.

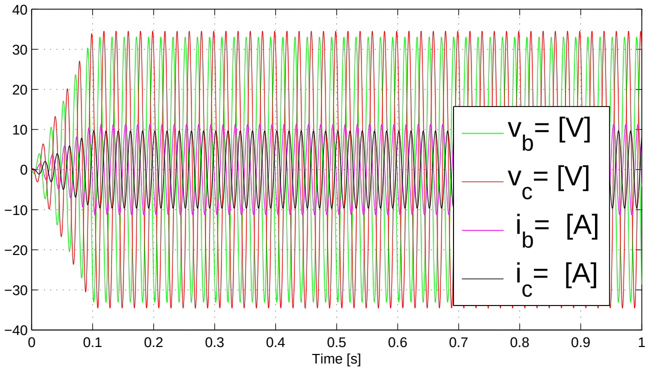

Figure 6.15: Result of simulation of two phase to ground short-circuit in phase b and c.

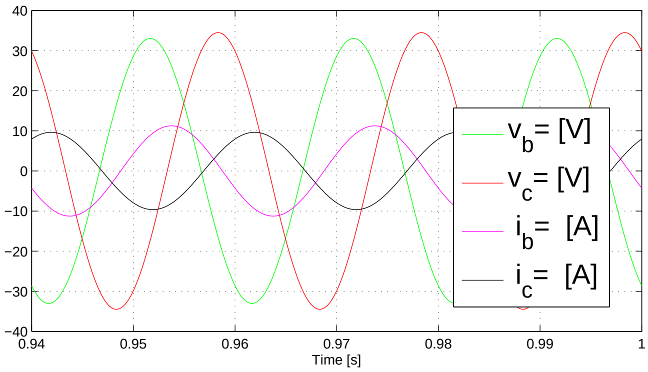

Figure 6.16: Zoom view of the result of simulation of two phase to ground short-circuit in phase b and c.

6.3.3 Three phase to ground short-circuit

The test set-up for this test can be seen in figure 6.17. This test is to calculate PPS and NPS components of the system since this type of error contains only PPS components.

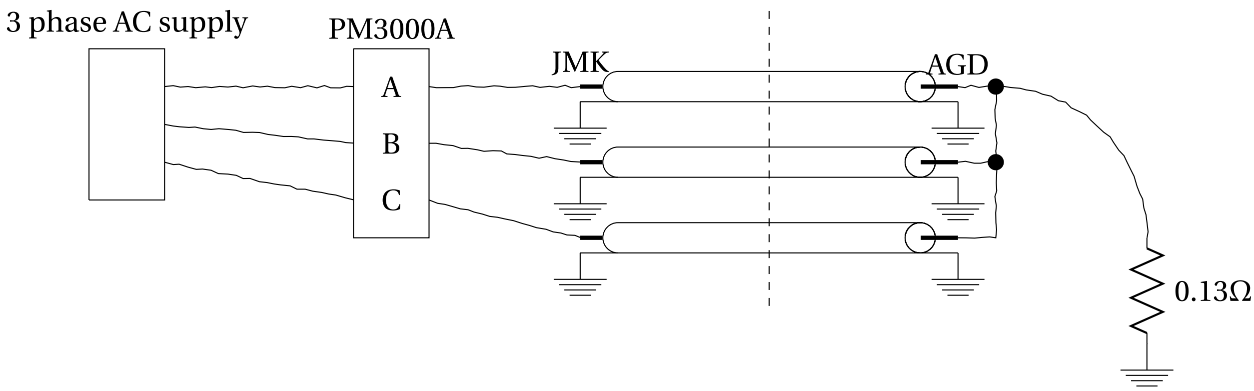

Figure 6.17: Test set-up of three phase to ground short-circuit.

The result of the three phase to ground short-circuit can be seen in figure 6.18, a zoom view of the steady state result can be seen in figure 6.19. The RMS values for the phase voltage have been set to $V_a = 23.70$, $V_b = 23.33$ and $V_c = 23.46$V and current has been calculated to be $I_a = 8.11\angle-53.1$A, $I_b = 8.01\angle-53.4$A and $I_c = 8.05\angle-52.9$A.

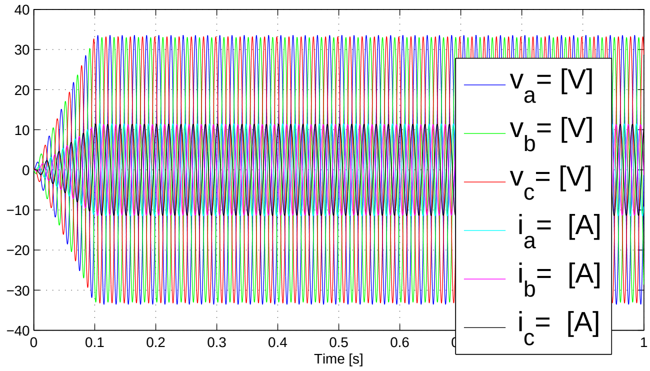

Figure 6.18: Result of simulation of three phase to ground short-circuit.

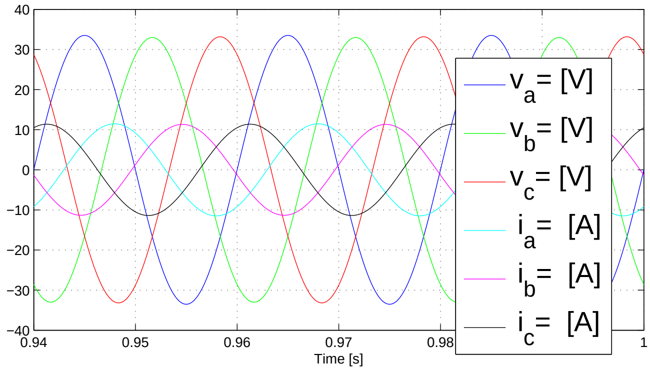

Figure 6.19: Zoom view of the result of simulation of three phase to ground short-circuit.

6.3.4 Zero phase sequence measurement

The test set-up for the ZPS measurement can be seen in figure 6.20.

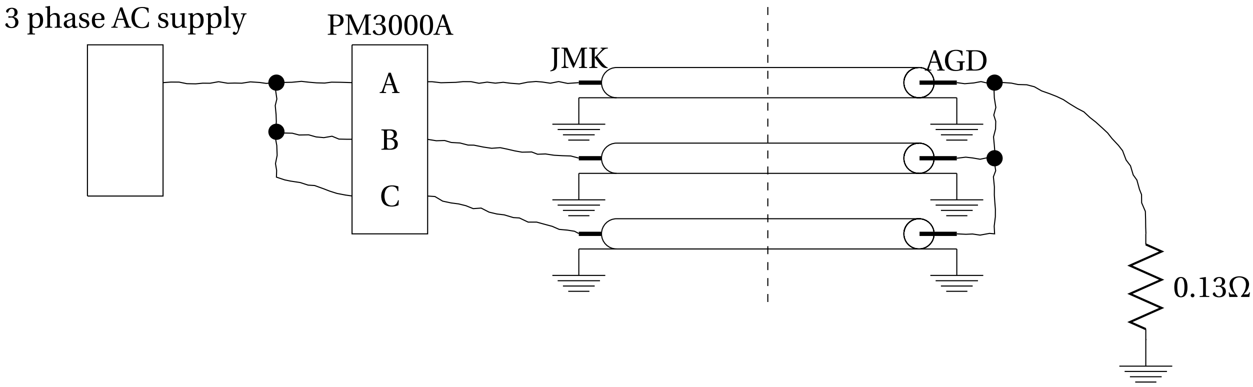

Figure 6.20: Test set-up of the ZPS measurement.

The result of the ZPS measurement can be seen in figure 6.21, a zoom view of the steady state result can be seen in figure 6.22. The RMS value for the phase voltage has been set to $V_Z = 18.34$V and current has been calculated to be $I_{Z_a} = I_{Z_b} = I_{Z_c} = 2.67\angle -30.6$A which sums up to $I_Z = 8.01\angle -30.6$A.

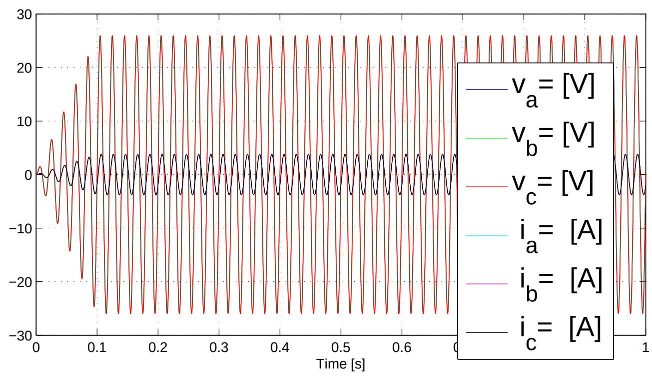

Figure 6.21: Result of simulation of ZPS measurement.

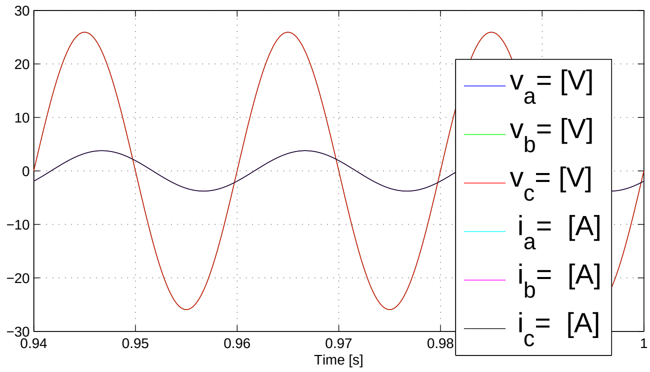

Figure 6.22: Result of simulation of ZPS measurement.

The summation of the ZPS current can be seen in figure 6.22 and 6.24.

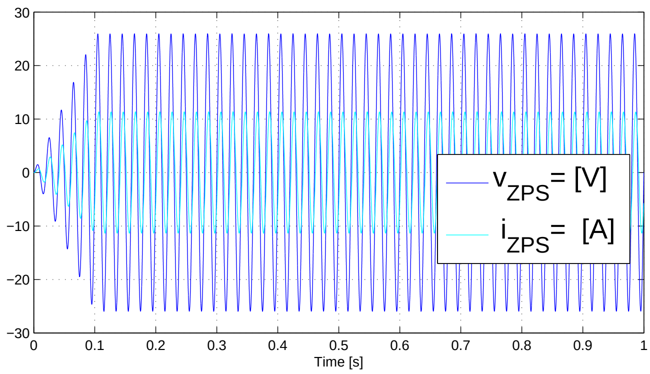

Figure 6.23: Result of simulation of ZPS measurement.

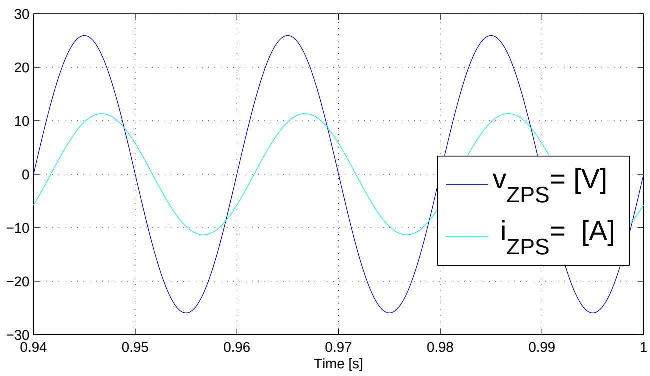

Figure 6.24: Result of simulation of ZPS measurement.

6.4 Expected results

Summation of the simulation results. All short-circuits are made to ground. The angle is from the voltage to the current.

Fault	Phase a			Phase b			Phase c		
	[V]	[A]	[°]	[V]	[A]	[°]	[V]	[A]	[°]
Phase a to ground	23.06	5.56	-41.4						
Phase b to ground				22.67	5.46	-39.6			
Phase c to ground							22.44	5.41	-41.4
Phase a and b to ground	22.84	7.81	-37.8	23.97	6.71	-63.0			
Phase a and c to ground	23.04	6.46	-64.8				22.21	7.56	-37.8
Phase b and c to ground				23.36	7.96	-37.8	24.39	6.82	-64.8
Three phase to ground	23.70	8.11	-52.2	23.33	8.01	-52.2	23.46	8.05	-54.0
ZPS	18.34	2.67	-30.6	18.34	2.67	-30.6	18.34	2.67	-30.6
ZPS sum	18.34	8.01	-30.6						

Table 6.1: Results of test simulation.

7 Field measurements

The purpose of the field measurements is to validate the the model made in PSCAD. Several measurements are made to create a basis for validation of the model in different scenarios. The description of the test set-up can be seen in section 6.2 on page 25.

7.1 Test results

The tests were conducted by supplying the cables through an auto transformer at JMK, and then making the short-circuits at AGD. During the tests the ground resistance was measured by Nyfors A/S in AGD to 0.13Ω.

7.1.1 Test equipment

The equipment used to perform the test on the system can be seen in table 7.1.

Type	Producer	Model	AAU Nr.	Specifications
Power analyzer	Voltech	PM3000A	29388	
Osciloscope	Tektronix	DPO2014		
Current probe	Tektronix	Tcp0030		Max 30A
Differential probe	Tektronix	P5200		
Auto transformer	Lübcke	RV 31002-20	89121	0-400/230V and 0-10A
DC voltage source	GWinstek	GPS-4303	87769	0-60V and 0-3A

Table 7.1: Equipment needed for the field measurements.

7.1.2 One phase to ground short-circuits

The one phase short-circuit was conducted according to the test set-up described in section 6.3.1 on page 27, with the following results which can be seen in figures 7.1 to 7.3.

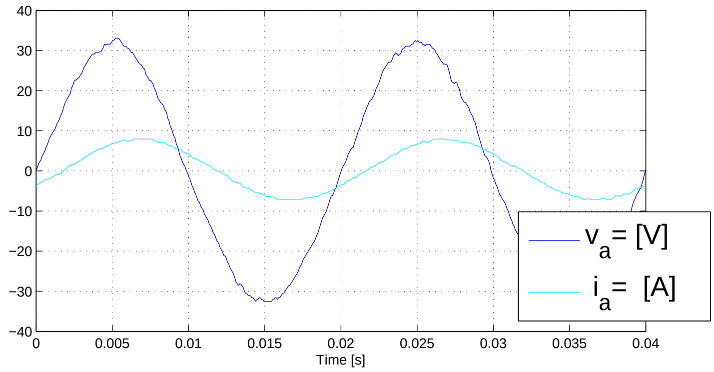

Figure 7.1: Result of measurement of one phase to ground short-circuit in phase a.

The short-circuit to ground in phase a was conducted with a voltage of 23.06V, and resulted in a current of $5.5230\angle -34.8$A.

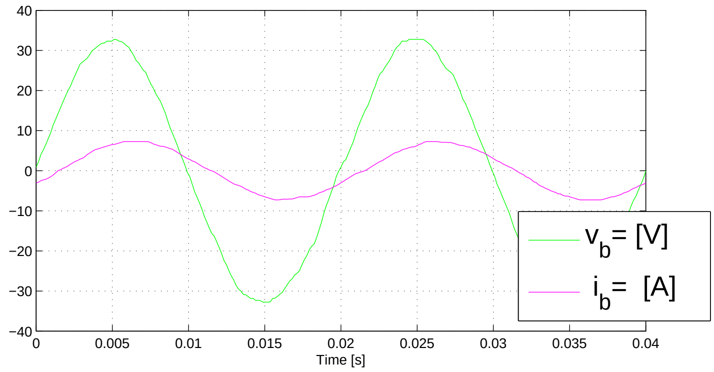

Figure 7.2: Result of measurement of one phase to ground short-circuit in phase b.

The short-circuit to ground in phase b was conducted with a voltage of 22.67V, and resulted in a current of $5.4325\angle -34.8$A.

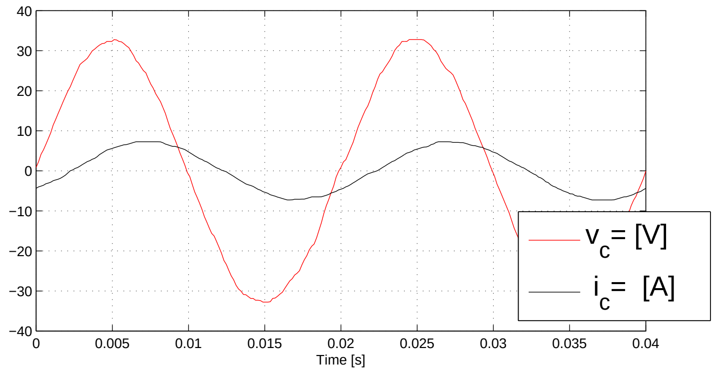

Figure 7.3: Result of measurement of one phase to ground short-circuit in phase c.

The short-circuit to ground in phase c was conducted with a voltage of 22.44V, and resulted in a current of $5.5215\angle -43.5$A.

7.1.3 Two phase to ground short-circuits

The two phase short-circuit was conducted according to the test set-up described in section 6.3.2 on page 29, with the following results which can be seen in figures 7.4 to 7.6.

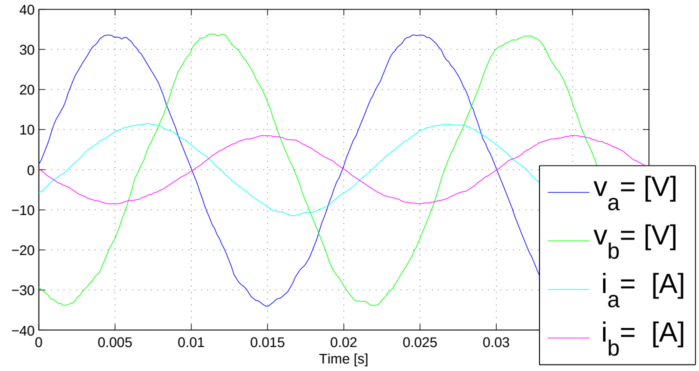

Figure 7.4: Result of measurement of Two phase to ground short-circuit in phase a and b.

The short-circuit to ground in phase a and b was conducted with a voltage of 22.84V in phase a and 23.97V in phase b, and resulted in a current of $8.1170\angle-34.2$A in phase a and $6.1470\angle-61.2$A in phase b.

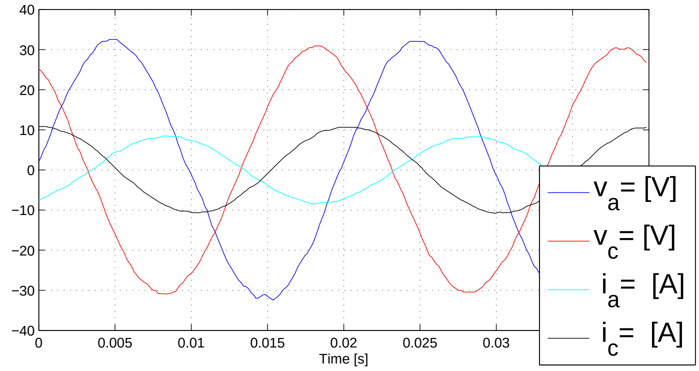

Figure 7.5: Result of measurement of Two phase to ground short-circuit in phase a and c.

The short-circuit to ground in phase a and c was conducted with a voltage of 23.04V in phase a and 22.21V in phase c, and resulted in a current of $6.0110\angle-65.68$A in phase a and $7.7590\angle-35.0$A in phase c.

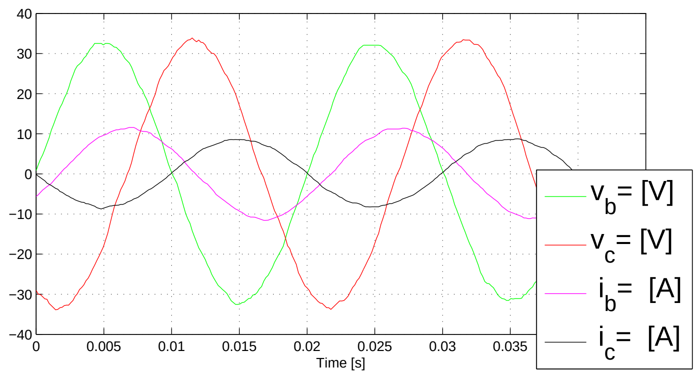

Figure 7.6: Result of measurement of Two phase to ground short-circuit in phase b and c.

The short-circuit to ground in phase b and c was conducted with a voltage of 23.36V in phase b and 24.39V in phase c, and resulted in a current of $8.2956\angle{-32.4}$A in phase b and $6.2815\angle{-61.2}$A in phase c.

7.1.4 Three phase to ground short-circuit

The three phase short-circuit was conducted according to the test set-up described in section 6.3.3 on page 32, with the following result which can be seen in figure 7.7.

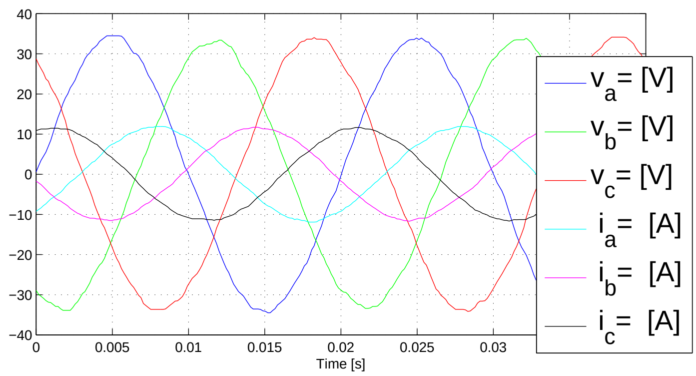

Figure 7.7: Result of measurement of three phase to ground short-circuit.

The three phase short-circuit to ground was conducted with a voltage of 23.70V in phase a, 23.33V in phase b and 23.46V in phase c, and resulted in a current of $8.1780\angle{-50.4}$A in phase a, $8.0595\angle-50.4$A in phase b and $8.0160\angle-55.5$A in phase c.

7.1.5 Zero phase sequence measurement

The ZPS measurement was conducted according to the test set-up described in section 6.3.4 on page 34, with the following result which can be seen in figure 7.8 and 7.9.

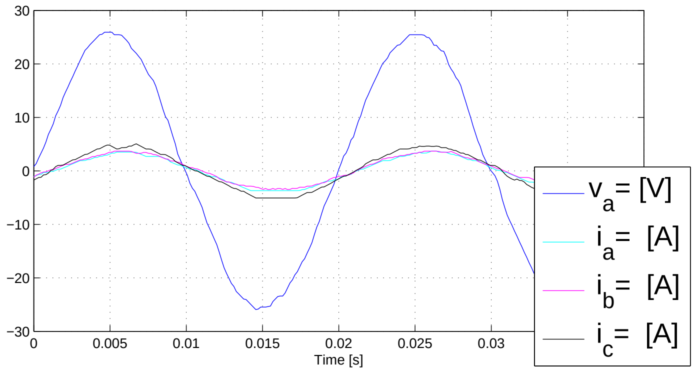

Figure 7.8: Result of the ZPS measurement.

The ZPS measurement was conducted with a voltage of 18.34V and resulted in a current of $2.6195\angle-15.4$Ain phase a, $2.6030\angle-19.0$A in phase b and $5.860\angle-11.8$A in phase c.

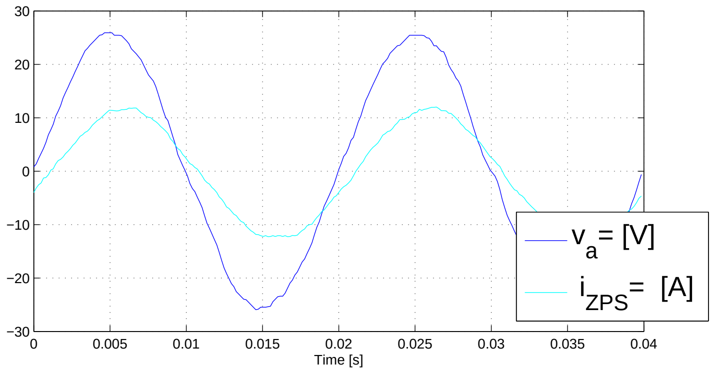

Figure 7.9: Result of the ZPS measurement.

The ZPS current is the sum of the phase currents in the ZPS measurement which gives a ZPS current of $7.8085\angle-15.4$A.

7.2 Summation of test results

The RMS values obtained with the power analyzer during the test. The tests were performed twice and the average values are listed below in table 7.2. The voltages measured deviated less than 1.5V per test and the current deviated less than 0.5 A per test.

Fault	Phase a			Phase b			Phase c		
	[V]	[A]	[°]	[V]	[A]	[°]	[V]	[A]	[°]
Phase a to ground	23.06	5.52	-34.8						
Phase b to ground				22.67	5.43	-34.8			
Phase c to ground							22.44	5.52	-43.5
Phase a and b to ground	22.84	8.12	-34.2	23.97	6.15	-61.2			
Phase a and c to ground	23.04	6.01	-65.6				22.21	7.76	-35.0
Phase b and c to ground				23.36	8.30	-32.4	24.39	6.28	-61.2
three phase to ground	23.70	8.18	-50.4	23.33	8.06	-50.4	23.46	8.02	-55.5
ZPS	18.34	2.62	-15.4	18.34	2.60	-19.0	18.34	2.59	-11.8
ZPS sum	18.34	7.81	-15.4						

Table 7.2: Average results of measurements in JMK.

By comparing the results from the model in table 6.1 on page 36 with the results from the measurements in table 7.2, this is don in table 7.3, it can be seen that the model is fairly correct in some cases, but not in all. Therefore some of the parameters in the model will be tested to see which parameters will result in changes in the cases where the model is inaccurate, and at the same time not give any change in the cases where the model is already accurate.
Table 7.3 shows the difference in currents and phase angle between the measurements and the simulation eg. "$test - sim$".

Fault	Phase a		Phase b		Phase c	
	[A]	[°]	[A]	[°]	[A]	[°]
Phase a to ground	-0.04	6.6				
Phase b to ground			-0.03	4.8		
Phase c to ground					0.11	-2.1
Phase a and b to ground	0.31	3.6	-0.56	1.8		
Phase a and c to ground	-0.45	-0.8			0.20	2.8
Phase b and c to ground			0.34	5.4	-0.54	3.6
three phase to ground	0.07	1.8	0.05	1.8	-0.08	-1.5
ZPS	-0.05	15.2	-0.07	11.6	-0.08	18.8

Table 7.3: Difference between the results of the measurements and the simulations.

8 Sensitivity analysis

The sensitivity analysis has been made to find out which parameters to adjust in order to make the model fit the measurements. As seen when comparing table 6.1 and 7.2 the PPS simulation corresponds well the measurement results, both in magnitude and phase angle. Whereas the ZPS simulation corresponds in magnitude but not in phase angle. Therefore it has been decided to test the model with both PPS and ZPS set-ups, in order to ensure that the model becomes valid in both cases. A conclusion and new values for the model are situated in section 8.6 on page 48.

The elements which will be tested in the sensitivity analysis are:

- Depth of cable
- Resistivity of:
  - Cable core
  - Cable screen
  - Ground (soil)
- Grounding impedance
- Permittivity of cable insulation
- Permeability of ground (soil)

Standard values for the model were: ground inductance = 0.001H, ground resistance = 0.13Ω, permeability of ground = 1, cable constants were as described in section 6.1 on page 23. The value for each parameter which were used in the model are marked with **bold** in the tables in the following sections.

8.1 Depth of cable

The depth of the cable has been checked, to see if it has any influence on the impedance of the cable. Two test cases have been examined, in the first one the cable is laid in a depth of 1.3m in the entire length of the cable. In the other test, the average depth of the under-drillings, as calculated in section 6.1.1 on page 23, is taken into consideration. This results in 18.012km with a depth of 1.3m and 696m with a depth of 2.8m.

Depth [m]	Current per phase [A]	Phase angle [°]
1.3	2.760	-29.82
1.3+2.8	2.671	-30.61

Table 8.1: Results of ZPS sensitivity analysis for cable depth.

Depth [m]	Phase a		Phase b		Phase c	
	[A]	[°]	[A]	[°]	[A]	[°]
1.3	8.113	-53.12	8.010	-53.35	8.049	-52.92
1.3+2.8	8.115	-53.11	8.011	-53.31	8.050	-52.88

Table 8.2: Results of PPS sensitivity analysis for cable depth.

As seen in table 8.1 the depth of the cable has an influence on the ZPS impedance, 3.33% in current magnitude. This parameter has almost no influence, less than 0.03%, on the PPS impedance as seen in table 8.2.

8.2 Resistivity

In this section the resistivity of the different parameters in the cable system is tested.

8.2.1 Resistivity of cable core

The resistivity of the cable core has been tested to see if small inaccuracies in the resistivity, due to impurities in the aluminum and temperature differences, would have any effect on the cable impedance. The resistivity for aluminum which is not cast or an alloy lies between 2.6 and 6.6[8].
The values for cable core resistivity chosen for test are: $2.6 \cdot 10^{-8}$ which is the resistivity for 99.99% pure aluminum, $2.8 \cdot 10^{-8}$ which is the resistivity for pure aluminum and $3.0 \cdot 10^{-8}\Omega\text{m}$ to see if the resistivity should be higher than the resistivity for pure aluminum.

Resistivity [Ωm]	Current per phase [A]	Phase angle [°]
$2.6 \cdot 10^{-8}$	2.706	-31.33
$\mathbf{2.8 \cdot 10^{-8}}$	2.671	-30.61
$3.0 \cdot 10^{-8}$	2.637	-30.44

Table 8.3: Results of ZPS sensitivity analysis for cable core resistivity.

Resistivity [Ωm]	Phase a		Phase b		Phase c	
	[A]	[°]	[A]	[°]	[A]	[°]
$2.6 \cdot 10^{-8}$	8.293	-55.31	8.187	-55.56	8.227	-55.11
$\mathbf{2.8 \cdot 10^{-8}}$	8.115	-53.11	8.011	-53.31	8.050	-52.88
$3.0 \cdot 10^{-8}$	7.942	-52.00	7.841	-52.22	7.878	-51.11

Table 8.4: Results of PPS sensitivity analysis for cable core resistivity.

As seen in table 8.3 small deviations in the core resistivity have some influence on the impedance of the cable. The deviation in the ZPS current is approximately 1.3% and the deviation in the PPS current is approximately 2.2% with a 7% deviation in resistivity.

8.2.2 Resistivity of cable screen

The resistivity of the cable screen has been tested, since this is a calculated value, and some assumptions were made to calculate the resistivity, the value could deviate from the calculated value. The values chosen for test are: $4.3835 \cdot 10^{-8}$, $4.8706 \cdot 10^{-8}$ and $5.3577 \cdot 10^{-8}\Omega$m.

Resistivity [Ωm]	Current per phase [A]	Phase angle [°]
$4.3835 \cdot 10^{-8}$	2.796	-31.39
$\mathbf{4.8706 \cdot 10^{-8}}$	2.671	-30.62
$5.3577 \cdot 10^{-8}$	2.554	-29.92

Table 8.5: Results of ZPS sensitivity analysis for cable screen resistivity.

Resistivity [Ωm]	Phase a		Phase b		Phase c	
	[A]	[°]	[A]	[°]	[A]	[°]
$4.3835 \cdot 10^{-8}$	8.141	-52.58	8.036	-52.78	8.076	-52.39
$\mathbf{4.8706 \cdot 10^{-8}}$	8.115	-53.12	8.011	-53.35	8.050	-52.92
$5.3577 \cdot 10^{-8}$	8.099	-53.50	7.997	-53.73	8.035	-53.30

Table 8.6: Results of PPS sensitivity analysis for cable screen resistivity.

Table 8.5 shows that the deviation in the current and phase angle is as much as 5% for the ZPS test and less than 0.5% for the PPS test, with a deviation in the resistivity of 10%.

8.2.3 Resistivity of ground

The soil in which the cable is laid contains loam, top soil and sandy soils. From [9] it can be seen that in the different types of soil the resistivity variates from 5 to 5000Ωm , so therefore it was decided to test at 10, 100 and 1000Ωm, which gave the following results.

Resistivity [Ωm]	Current per phase [A]	Phase angle [°]
10	2.677	-31.13
100	2.671	-30.62
1000	2.664	-30.26

Table 8.7: Results of ZPS sensitivity analysis for soil resistivity.

Resistivity [Ωm]	Phase a		Phase b		Phase c	
	[A]	[°]	[A]	[°]	[A]	[°]
10	8.116	-53.14	8.012	-53.33	8.051	-52.91
100	8.115	-53.12	8.011	-53.31	8.049	-52.8
1000	8.114	-53.16	8.010	-53.36	8.050	-52.92

Table 8.8: Results of PPS sensitivity analysis for soil resistivity.

From table 8.7 and 8.8 it can be seen that the soil resistivity does not have much influence on the results of the simulations, even though the resistivity was changed by a factor of 10 the results only deviated less than 0.3% for both the ZPS and the PPS test.

8.3 Ground impedance

The ground impedance has been measured by Nyfors A/S to 0.13Ω. In the sensitivity analysis this is assumed to be the total impedance, so the angle of the impedance has been tested. The values for the inductive part of the impedance were set to be 0.00005 0.0001, 0.0002 and 0.001H, and the resistive part was calculated from these values. The 0.001H were chosen when creating the model, since this were assumed to be a small inductance. The ground resistance have also be set to 0.13Ω with an inductance of 0H to test what would happen if the ground impedance was purely resistive.

Inductance [H]	Resistance [Ω]	Current per phase [A]	Phase angle [°]
0.0	0.130	2.888	-18.21
0.00005	0.129	2.883	-18.61
0.0001	0.126	2.886	-19.40
0.0002	0.114	2.915	-20.97
0.001	0.130	2.671	-30.62

Table 8.9: Results of ZPS sensitivity analysis for ground impedance.

Inductance [H]	Resistance [Ω]	Phase a		Phase b		Phase c	
		[A]	[°]	[A]	[°]	[A]	[°]
0.0	0.130	7.989	-53.67	7.883	-53.97	7.928	-53.44
0.00005	0.129	7.994	-53.00	7.890	-53.24	7.934	-52.82
0.0001	0.126	8.000	-53.00	7.896	-53.22	7.941	-52.79
0.0002	0.114	8.014	-53.00	7.909	-53.24	7.953	-52.80
0.001	0.130	8.115	-53.12	8.011	-53.31	8.049	-52.88

Table 8.10: Results of PPS sensitivity analysis for ground impedance.

It can be seen from table 8.9, that the ground resistance has a high impact on the ZPS result, compared to the things previously tested, as much as 10% in current magnitude and 40% in phase angle. In table 8.10 it can be seen that in the PPS test the change in ground resistance gives a 1.5% change in the magnitude of the current and a 0.2% change in the phase angle.

The difference between the 2 tests can be explained from the ground return current, which is approximately 7.8A in the ZPS test, and only approximately 50mA in the PPS test.

As it can be seen from table 8.9 and 8.10, the test in which the ground impedance is purely resistive, gives lower results regarding the phase angle. In the ZPS test the rest of the results are higher than the results for a ground inductance of 50μH.

8.4 Permittivity of cable insulation

The permittivity is a calculated parameter. In order to be able to calculate the value some assumptions have been made. This value has been tested to see if small deviations in the value have any impact on the results. A decision was made to test the values: 2.1816, 2.6816 and 3.1816Ωm.

Permittivity	Current per phase [A]	Phase angle [°]
2.1816	2.660	30.69
2.6816	2.671	30.62
3.1816	2.679	30.53

Table 8.11: Results of ZPS sensitivity analysis for insulation permittivity.

Permittivity	Phase a		Phase b		Phase c	
	[A]	[°]	[A]	[°]	[A]	[°]
2.1816	8.053	53.24	7.950	53.43	7.989	53.03
2.6816	8.115	53.12	8.011	53.35	8.050	52.92
3.1816	8.170	52.99	8.065	53.17	8.104	52.81

Table 8.12: Results of PPS sensitivity analysis for insulation permittivity.

It can be seen in table 8.11 and 8.12, that a 18% deviation in the permittivity gives a deviation in the current and phase angle of less than 1% for both the ZPS and PPS test.

8.5 Permeability of ground

The permeability of the soil was tested. This value can have small deviations due to the surroundings.

It was decided to test with the relative permeability of water, in order to get an absolute minimum permeability for moist soil. The relative permeability was calculated from $\mu_r = \chi + 1$, where $\chi_{water} = -0.9 \cdot 10^{-5}$[10], this gives a permeability of 0.999991.

The relative permeability of dry soil was calculated by $\chi = 30.3 \cdot 10^{-6}$[11], which gives a permeability of 1.00003.

Permeability	Current per phase [A]	Phase angle [°]
0.999991	2.6715	30.61
1.0	2.6713	30.62
1.00003	2.6731	30.69

Table 8.13: Results of ZPS sensitivity analysis for soil permeability.

Permeability	Phase a		Phase b		Phase c	
	[A]	[°]	[A]	[°]	[A]	[°]
0.999991	8.116	53.11	8.013	53.42	8.051	52.86
1	8.115	53.12	8.011	53.35	8.050	52.92
1.00003	8.123	53.13	8.020	53.29	8.028	52.95

Table 8.14: Results of PPS sensitivity analysis for soil permeability.

From table 8.13 and 8.14 it can be seen, that the soil permeability has some influence even with small deviations. From moist to dry soil, the results deviate with up to 0.3% with a deviation in permeability of 0.0039%.

8.6 Conclusion and new values

The depth of the cable has some influence on the ZPS impedance, so even though the influence is small, it is considered more accurate to include the underdrillings in the model.

The most significant change in the results for the ZPS phase angle was the ground impedance. The ground resistance was measured by Nyfors A/S to 0.13Ω. This was assumed to be the DC part of the ground impedance for the original model. In the sensitivity analysis this assumption was changed to a total impedance of 0.13Ω. Therefore the ground inductance has been set to 50μH and the ground resistance has been set to 0.129Ω.

By increasing the resistivity of the screen the current in the ZPS test dropped, more than the PPS current. This change has been taken into consideration since the ZPS current was higher in the model than in the test. The resistivity of the screen was set to $5.3577 \cdot 10^{-8}$Ωm.

When the change in the ground impedance and the cable screen resistivity was implemented the PPS current dropped. Consequently it was considered which parameter would give a higher PPS current without changing the ZPS results. The parameter which could do this is the cable core resistivity. By lowering the resistivity the PPS current increased significantly compared to the ZPS current. Therefore the resistivity was changed to 2.6Ωm from 2.8Ωm.

The resistivity of the soil had almost no influence even with major changes in the values, so this will not be changed from the original model.

In order for the cable insulation permittivity to have any influence on the results the changes should be significant, and therefore the permittivity will not be changed.

Even though the soil permeability gives major changes in the results compared to the change in permeability, the deviations are still small compared to the other results. In order to give these results any significance the change has to be bigger than probable.

8.6.1 New values

The sensitivity analysis led to a decision to use the values in the model shown in table 8.15.

Parameter	Value	Unit
Depth	1.3+2.8	[m]
Resistivity of core	$2.6 \cdot 10^{-8}$	[Ωm]
Resistivity of screen	$5.3577 \cdot 10^{-8}$	[Ωm]
Resistivity of soil	100	[Ωm]
Ground inductance	0.00005	[H]
Permittivity of insulation	2.6816	[−]
Permeability of soil	1	[−]

Table 8.15: Parameters to use in the model.

Results after new values have been implemented, can be seen in table 8.16.

Fault	Phase a			Phase b			Phase c		
	[V]	[A]	[°]	[V]	[A]	[°]	[V]	[A]	[°]
Phase a to ground	23.06	5.88	-36.0						
Phase b to ground				22.67	5.78	-36.0			
Phase c to ground							22.44	5.72	-36.1
Phase a and b to ground	22.84	8.27	-38.8	23.97	6.31	-66.5			
Phase a and c to ground	23.04	6.07	-66.6				22.21	8.01	-38.8
Phase b and c to ground				23.36	8.43	-38.8	24.39	6.41	-66.5
Three phase to ground	23.70	8.17	-54.9	23.33	8.06	-55.0	23.46	8.11	-54.7
ZPS	18.34	2.61	-18.2	18.34	2.61	-18.2	18.34	2.61	-18.2
ZPS sum	18.34	7.83	-18.2						

Table 8.16: Results of the test after new values have been implemented.

As seen in table 8.16, when compared to table 6.1 and 7.2 that the results from simulation with the new values are more correct in most cases.

Table 8.17 shows the difference in currents and phase angle between the measurements and the simulation eg. "$test - sim$". Since the simulation were done with the same voltages as the measurements the voltages have been left out of this table.

Fault	Phase a		Phase b		Phase c	
	[A]	[°]	[A]	[°]	[A]	[°]
Phase a to ground	-0.36	1.2				
Phase b to ground			-0.35	1.2		
Phase c to ground					-0.2	-7.4
Phase a and b to ground	-0.15	4.6	-0.16	5.3		
Phase a and c to ground	-0.06	1.0			0.25	3.8
Phase b and c to ground			-0.13	6.4	-0.13	5.3
three phase to ground	0.01	4.5	0.00	4.6	-0.09	-0.8
ZPS	0.01	2.8	-0.01	-0.8	-0.02	6.4

Table 8.17: Difference between the results of the measurements and the simulations with the new values implemented.

9 Validation of standard formula

The PPS and ZPS impedance is used in the setting of distance protection relays, therefore the impedances will be calculated in this chapter.

9.1 Standard formula

Nyfors A/S calculate the ZPS impedance as three times the PPS impedance[5] this will be referred to as the standard formula. The $Z_{PPS_{std}}$ is calculated with equation 9.3, the calculations done by Nyfors A/S can be seen on the CD in: E:\Nyfors AS\Beregning af indstillinger JMK2AGD.pdf.

$$R_{DC} = 0.0778 \cdot 18.708 = 1.4555 \qquad [\Omega] \quad (9.1)$$

$$X_{50\text{Hz}} = 0.133 \cdot 18.708 = 2.4882 \qquad [\Omega] \quad (9.2)$$

$$Z_{PPS_{std}} = R_{DC} + \jmath \cdot X_{50\text{Hz}} \qquad [\Omega]$$

$$\downarrow$$

$$Z_{PPS_{std}} = 1.4555 + \jmath \cdot 2.4882 = 2.8826\angle 59.67 \qquad [\Omega] \quad (9.3)$$

The calculation of the standard formula can be seen in equation 9.4, the result of the standard formula will be named $Z_{ZPS_{std}}$.

$$Z_{ZPS_{std}} = Z_{PPS_{std}} \cdot 3 \qquad [\Omega]$$

$$\downarrow$$

$$Z_{ZPS_{std}} = 2.8826\angle 59.67 \cdot 3 = 8.6478\angle 59.67 \qquad [\Omega] \quad (9.4)$$

9.2 PPS impedance

The PPS impedance can be calculated with equation 9.5[3].

$$Z_{PPS} = \frac{V_{PPS}}{I_{PPS}} \qquad [\Omega] \quad (9.5)$$

The PPS voltage used in the test is 23.50V and the current measured is $8.09\angle -52.1$A are the average values from the test , this gives a PPS impedance as calculated in equation 9.6.

$$Z_{PPS} = \frac{23.50}{8.09\angle -52.1} = 2.91\angle 52.1 \qquad [\Omega] \quad (9.6)$$

It can be seen from equation 9.3 and 9.6 that the magnitude of the PPS impedance, calculated with the standard formula, deviates less than 1% from the actual PPS impedance calculated from the measurements. The deviation between the standard formula and the measurements can be explained from the fact that the standard formula, does not take ground impedance into consideration.

9.3 ZPS impedance

The correct way to calculate the ZPS impedance is with equation 9.7[3].

$$Z_{ZPS} = \frac{3 \cdot V_{ZPS}}{I_{ZPS}} \quad [\Omega] \quad (9.7)$$

The ZPS voltage and current that were used/measured in the measurements can be found in table 7.2 on page 42 and are stated here for revision purposes $V_{ZPS} = 18.34$V and $I_{ZPS} = 7.81\angle-15.04$A. The Z_{ZPS} has been calculated to be 7.04Ω, which can be seen in equation 9.8.

$$Z_{ZPS} = \frac{3 \cdot 18.34}{7.81\angle-15.04} = 7.04\angle 15.04 \quad [\Omega] \quad (9.8)$$

From equation 9.8 and 9.4 it can be seen that the standard equation gives a result, which is 22% higher than the actual ZPS impedance calculated from measurements.

In equation 9.9 the ZPS impedance has been calculated from the simulation results.

$$Z_{ZPS} = \frac{3 \cdot 18.34}{7.83\angle-18.2} = 7.02\angle 18.2 \quad [\Omega] \quad (9.9)$$

From equation 9.9 it can be seen that a simulation results generates a value for the ZPS impedance which are close to the real value calculated from the measurements, compared to the standard equation.
The standard equation calculates the ZPS impedance with guidelines meant for OHL[5]. As it can be seen from the sensitivity analysis in chapter 8 different parameters have influence on the ZPS currents without much influence on the PPS currents. Consequently, if some of these parameters change slightly the calculation, in which the PPS impedance is multiplied by a factor in order to get the ZPS impedance, must be considered inaccurate.

10 *Finite Element Method modeling*

The Finite Element Method (FEM) model is used to determine the magnetic and electrical fields around the cable. The FEM model is created with COMSOL Multiphysics.

10.1 Parameter determination

When the model is created, the types of physics have to be chosen. In this model it has been chosen to use electrostatics and magnetic fields. After choice of physics, some different parameters have to be set, the parameters chosen for use in this model are: materials, geometry and the electric potentials of the cables.

10.1.1 Materials

The first thing to do, is to determine, which types of material are used in the system.

- Aluminum - used in the core of the cable.
- Insulating material 1 - used as insulator between core and screen.
- Copper - used for screen (with a calculated resistivity).
- Insulation material 2 - used as the outer insulation of the cable.
- Soil - the soil surrounding the cable.

COMSOL Multiphysics has a build-in material library, where some materials can be found. Here aluminum and copper are found, whereas values for the insulation materials, soil and the resistivity for the copper have been taken from the PSCAD model. The values which are used to define the insulating materials and the soil in COMSOL Multiphysics are permittivity, permeability and electrical conductivity. The values of these parameters can be seen in table 10.1 together with the conductivity for the screen.

	Permittivity	Permeability	Conductivity
Insulator 1	2.6816	1	0
Insulator 2	2.3	1	0
Screen			2.05314e7
Soil	1	1	0.01

Table 10.1: The values of the parameters used in the FEM model.

10.1.2 Geometry

The next thing to do is to define the geometry. This is done by defining each layer of the cable as a circle with a radius equal to the outer radius of the layer, and the thickness equal to $r_o - R_i$, the setting of circle one can be seen in figure 10.1. The only difference is the cable core, which has been set to the type solid and the ground (soil), which has been created by a 2.6m square.

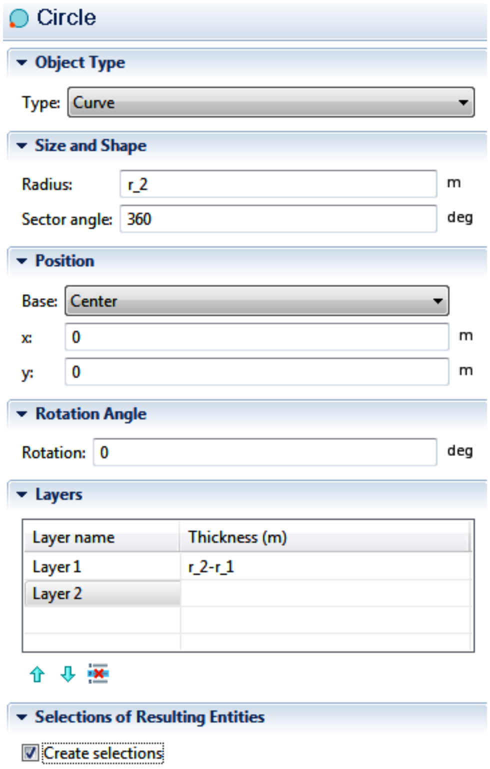

Figure 10.1: Figure of the geometry settings panel in COMSOL Multiphysics.

When the geometry has been created COMSOL Multiphysics can create a mesh for the calculations. The geometry and the mesh can be seen in figure 10.2.

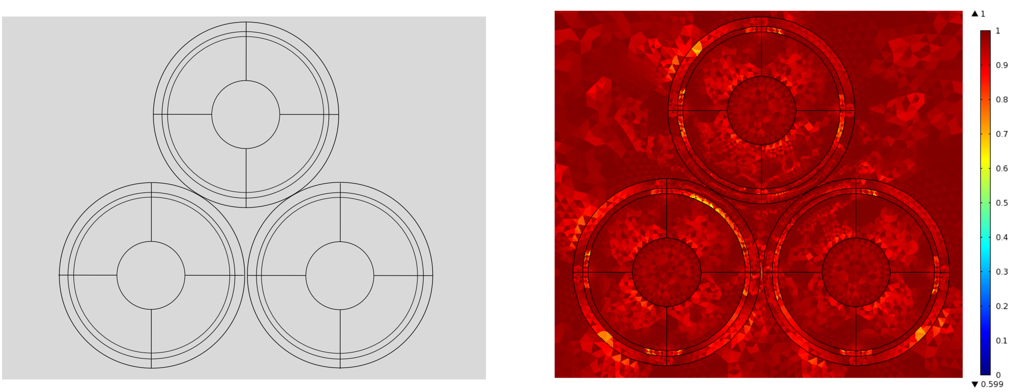

Figure 10.2: Left: The geometry as created in COMSOL Multiphysics. Right: The mesh created by COMSOL Multiphysics.

10.2 Results of the FEM analysis

In this section the results of the FEM analysis will be described. It has been decided to make two analyses in which the voltage and current are set as in the measurements of the three phase short-circuit (PPS measurement) and of the ZPS measurement.

10.2.1 Three phase short-circuit

Voltage angle of phase a = 0°

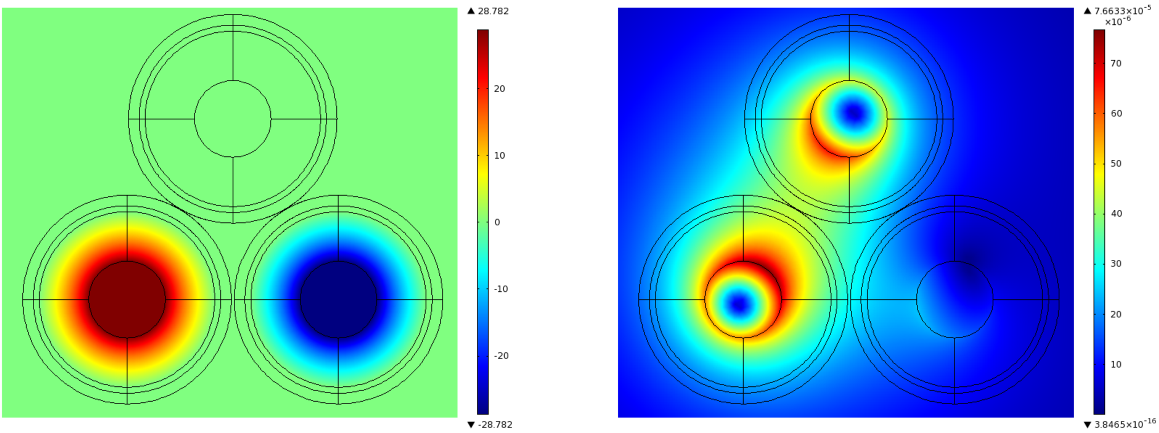

Figure 10.3: Left: Electrical field. Right: Magneticfield.

It can be seen from figure 10.3 that the voltage potential of phase a is equal to 0V, at this time the value for the current of phase a is -2.83A. The values for phase b and c are $v_b = -28.78$V, $v_c = 28.78$V, $i_b = -0.614$A and $i_c = 3.45$A. This gives a magnetic coupling primarily between phase a and c since the current in phase b is close to 0 and therefore only creates some distortion of the magnetic field. Phase a and c pull on each other since the current of phase a is negative and in phase b the current is positive.

Current angle of phase a = 0°

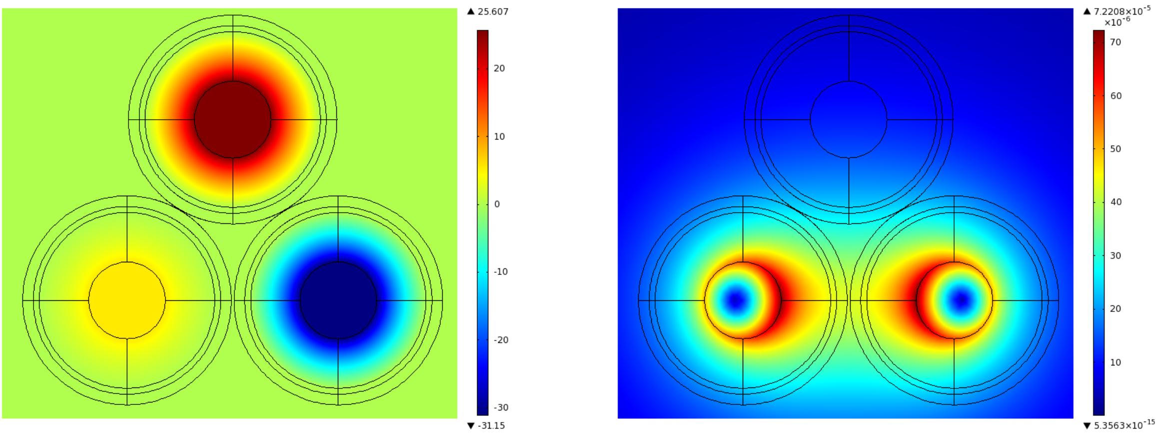

Figure 10.4: Left: Electrical field. Right: Magneticfield.

In this example the current in phase a is equal to 0, this gives a voltage angle equal to 50.4°and a voltage of 25.61V. The values for phase b and c at this time are $v_b = -31.15$V, $v_c = 5.542$V, $i_b = -3.188$A and $i_c = 3.188$A. This gives a magnetic field between phase b and c without any distortion from phase a, as seen in figure 10.4.

Voltage angle of phase a = 90°

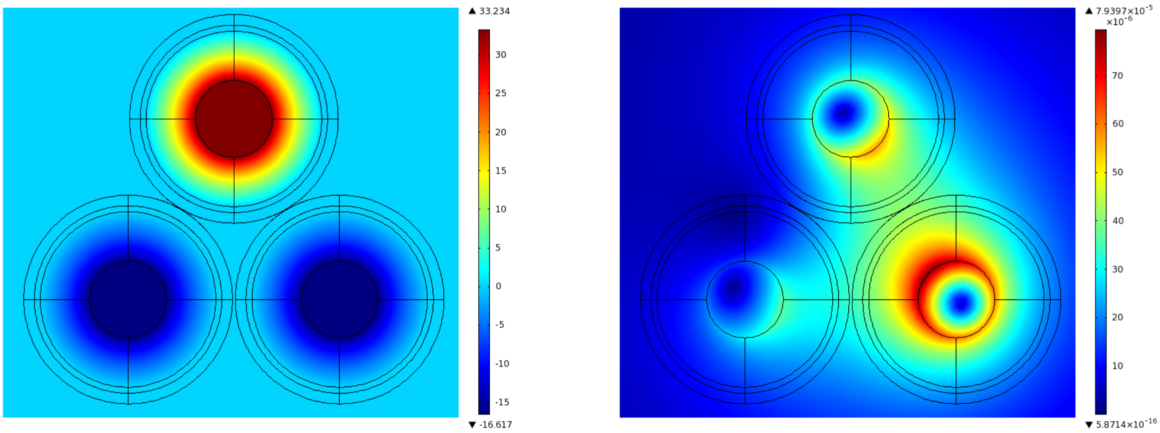

Figure 10.5: Left: Electrical field. Right: Magneticfield.

It can be seen from figure 10.5 that the voltage potential of phase a is in 90° angle, peak value, this gives a voltage equal to 33.23V, at this time the value for the current of phase a is -2.346A. The values for phase b and c are $v_b = v_c = -16.62$V, $i_b = -3.63$A and $i_c = 1.283$A. From this it can be seen that the primary coupling is between phase a and b, since the current in phase c is the one closest to 0.

Current angle of phase a = 90°

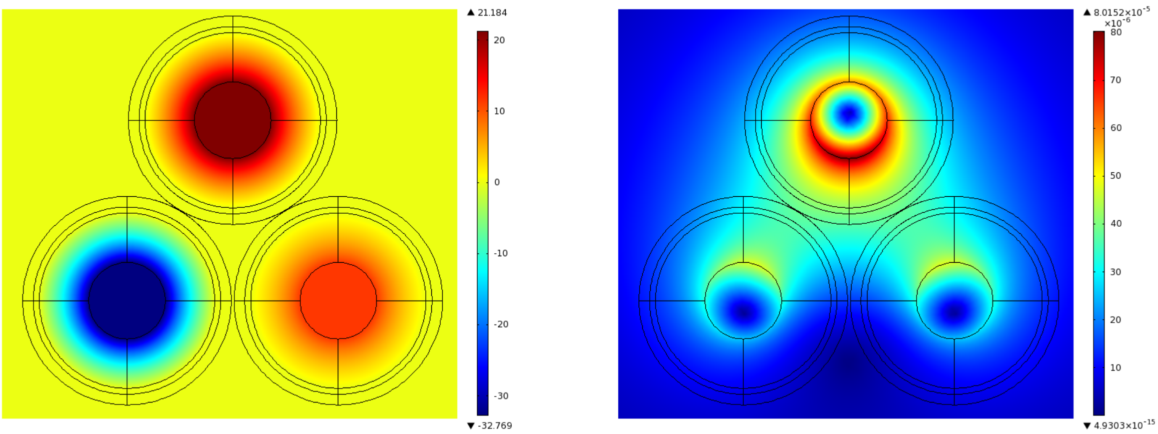

Figure 10.6: Left: Electrical field. Right: Magneticfield.

It can be seen from figure 10.6 that the current in phase a is in 90° angle, peak value, this gives a current equal to 3.681A, at this time the value for the voltage of phase a is 21.18V.

The values for phase b and c are $v_b = 11.58$ and $v_c = -32.77$V, $i_b = i_c = -1.841$A. from this it can be seen, in figure 10.6, that the magnetic field is distributed from phase a and equally towards phase b and c. The magnetic field is pulling phase a directly in between phase b and c, this is due to the positive current in phase a and negative current in b and c.

10.2.2 Zero phase sequence

Voltage angle of phase a = 0°

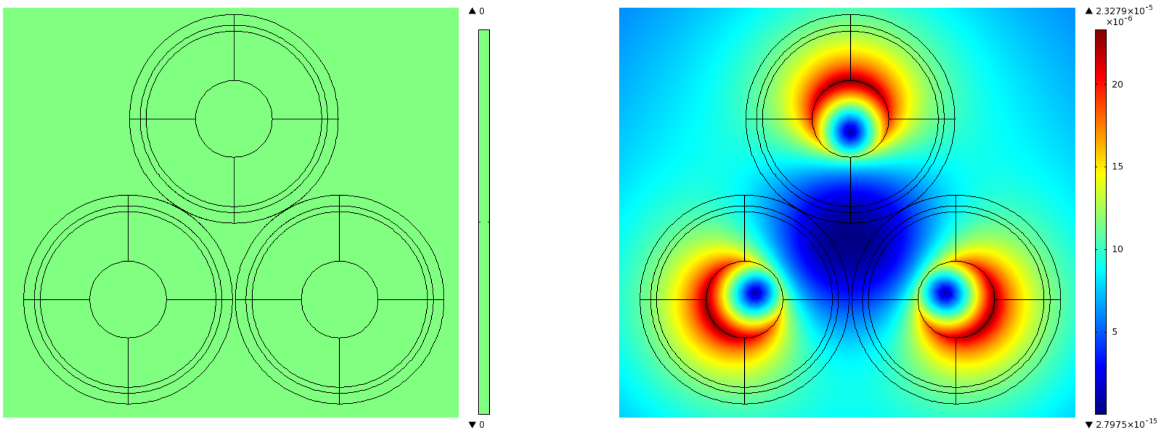

Figure 10.7: Left: Electrical field. Right: Magneticfield.

From figure 10.7 it can be seen, that the voltage of all phases is 0, since the current is lagging by 15.4° the current is -0.978A in all phases.

Current angle of phase a = 0°

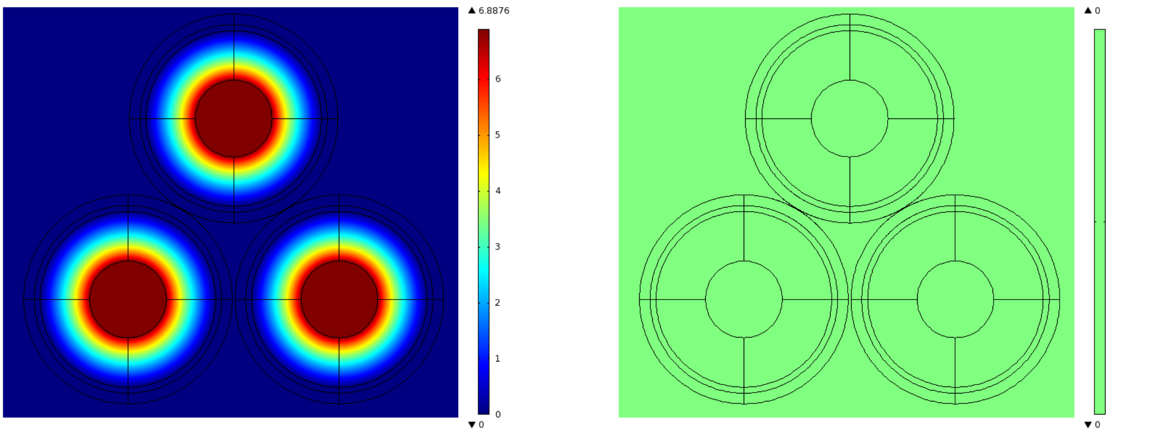

Figure 10.8: Left: Electrical field. Right: Magneticfield.

In figure 10.8 it can be seen that there is no magnetic field. This is due to the current being 0A. Due to the 15.4° current lag, the voltage is 6.888V in each phase.

Voltage angle of phase a = 90°

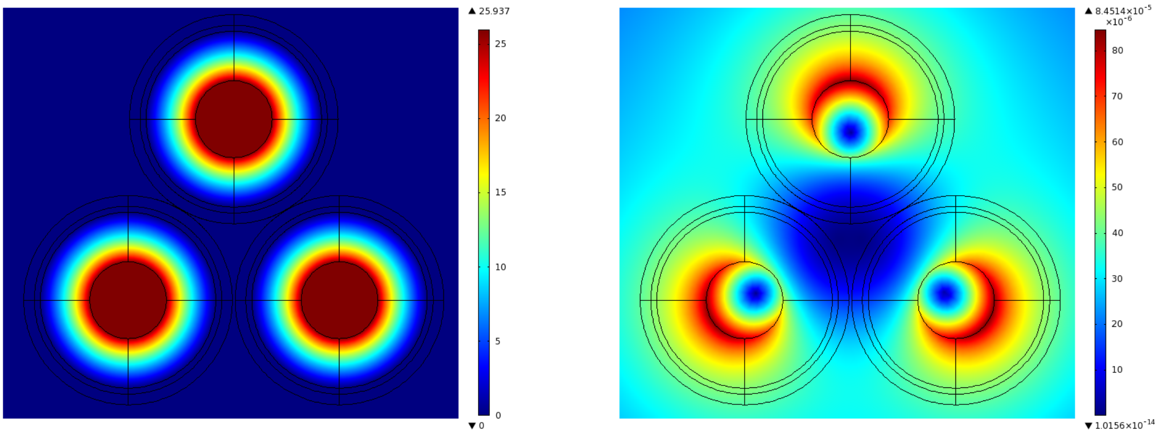

Figure 10.9: Left: Electrical field. Right: Magneticfield.

In figure 10.9 the voltage is 25.94V, and the current is 3.552A in all phases.

Current angle of phase a = 90°

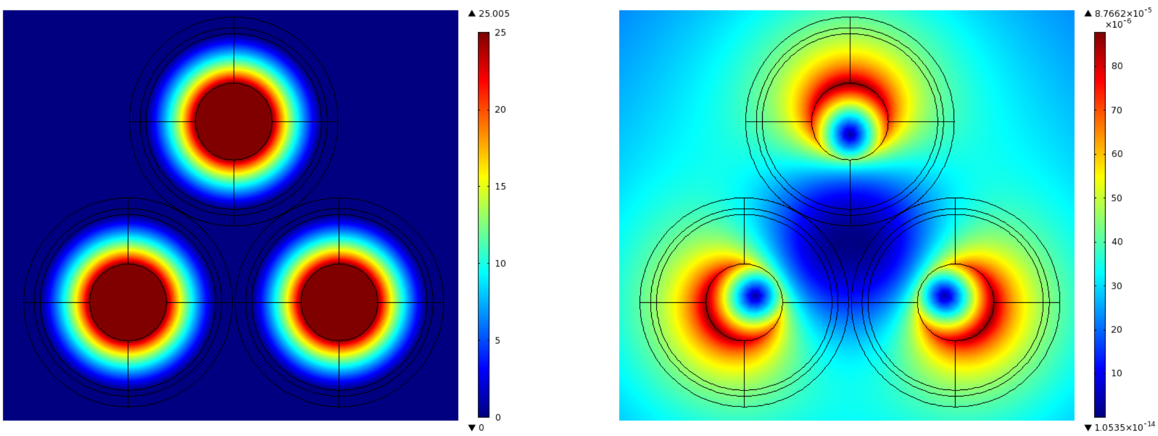

Figure 10.10: Left: Electrical field. Right: Magneticfield.

In figure 10.10 the current is at peak, 3.684A.The voltage is 25.01V.

10.3 Conclusion

This analysis has shown that the electric field is in all cases are contained inside each cable, and are not influenced by the change between PPS and ZPS currents.

The magnetic field is influenced by the change between PPS and ZPS as expected. The change in the magnetic field can explain the influence by the soil permeability, which were discovered in the sensitivity analysis in chapter 8. The change can be explained by the fact that the current in the PPS sensitivity analysis is higher than the current in the ZPS analysis, which makes the magnetic field stronger and therefore, the influence of the permeability of the soil have a higher influence.

11 Conclusion and guidelines

From the measurements and the PSCAD model, the actual PPS and ZPS impedances have been calculated in order to see if the guidelines used today, which originally were meant for OHL, can be used for cables or if they have to be updated.

From the sensitivity analysis it has been discovered that the ZPS and PPS currents were not dependent on the same parameters. for example The ZPS currents were dependent on: the depth of the cable, the resistivity of the cable screen and the ground impedance. The PPS current, on the other hand was dependent on the resistivity of the cable core.

From the FEM analysis it could be seen that the electric- and magnetic fields behaved as expected. The electric field was contained inside each cable (between core and screen). The magnetic field was on the other hand not contained by the cable screen, and was influenced by the change between PPS and ZPS currents.

11.1 Guidelines

In chapter 9 it was seen that the PPS impedance calculation done by Nyfors A/S is valid so this needs no changing in method.

The calculation of the ZPS impedance resulted in a ZPS impedance calculated from the measurements which had a factor 2.44 in magnitude of the PPS calculated by Nyfors A/S. The angle of the ZPS impedance was only one fourth of the angle of the PPS impedance. The difference in the factors for magnitude and angle can be due to that the ZPS impedance is highly dependent on the ground impedance, whereas the PPS impedance is almost not influenced by the ground impedance. The guideline used by Nyfors A/S today uses a factor 3 on the PPS impedance to calculate the ZPS impedance. The result of this is that the formula for calculation of the ZPS impedance needs tuning for ground impedance and other parameters.

The way to measure the ZPS impedance is simple, the equipment needed for the measurements are: a one phase power supply, voltage-, current- and phase angle measurement devices.

It must be recommended to measure the cable or create a model of the cable, in order to obtain the ZPS impedance.

12 *Future work*

The next thing this project should do is to obtain more measurements of PPS and ZPS currents in other cables. The new measurements should be used as a statistical basis for new standards to calculate the ZPS impedance from the calculated PPS impedance.

The laying profiles should also be looked into to see if the PPS and ZPS impedance changes if the three cables are laid in flat formation instead of trefoil.

The ground conditions could also be more thoroughly investigated, this being both the ground impedance and the soil parameters, such as resistivity and permeability.

13 Bibliography

[1] Kabellægning af 132 og 150 kilovolt net, 2009. URL `http://energinet.dk/DA/ANLAEG-OG-PROJEKTER/Anlaegsprojekter-el/Sider/Kabellaegning-af-132-og-150-kilovolt-net.aspx`.

[2] J.C. Das. *Power system analysis: short-circuit load flow and harmonics*. Marcel Dekker, 2002. ISBN 9780824707378.

[3] N.D. Tleis. *Power systems modelling and fault analysis: theory and practice*. Newnes power engineering series. Newnes, 2007. ISBN 9780750680745.

[4] William A. Thue, editor. *Electrical Power Cable Engineering*. Marcel Dekker, Inc., 1999. ISBN 0-8247-9976-3.

[5] Danske Elværkers Forenings Udredningsafdeling. *Afstandsrelæer i slukkespolejordede 50-60 kV net*. Komitérapport / DEFU. Dansk Energi, 1990.

[6] Unnur Stella Guðmundsdóttir. *Modelling of long High Voltage AC cables in Transmission Systems*. PhD thesis, Aalborg University, Department of Energy Technology, June 2010.

[7] Christian Flytkær Jensen. Studies of transient overvoltage at the horns rev 2 wind farm hvac cable connection. Technical report, Aalborg University, Department of Energy Technology, 2009.

[8] Brian Larson. Conductivity and resistivity values for aluminum & alloys, 2002. URL `http://www.ndt-ed.org/GeneralResources/MaterialProperties/ET/et_matlprop_index.htm`.

[9] M.N. Fikri Bin Razali and S.B. Azahar bin Syed Osman. Non-quantitative correlation of soil resistivity with some soil parameters. In *National Postgraduate Conference (NPC), 2011*, pages 1 –4, sept. 2011. ISBN 978-1-4577-1882-3. doi: 10.1109/NatPC.2011.6136365.

[10] Richard Alexander Clarke. Magnetic properties of materials, 2008. URL `http://info.ee.surrey.ac.uk/Workshop/advice/coils/mu/#sus`.

[11] V. S. Semenov and V. I. Pakhotnova. An investigation of the magnetic properties of soils. *Russian Physics Journal*, 41(7):656–661, 1998.

III APPENDIX

A Data-sheet

Medium and high voltage cables	Units	Item
Cable code		0343895
Cable type		TSLE
Standard		IEC 60840
Standard		Esp. Cliente
Nominal voltage (PG/LL)	kV	47/72
No of cores × C.S.A.	N×mm^2	1x400
Conductor material		AL
Shape		Circular
Class/standard		1/EN 60228
Nominal diameter	mm	21.60
W.B. conductor		No
Swellable semi-conducting tape over conductor		No
Conductor screen material		Extruded semi-conducting layer
Nominal radial thickness	mm	0.8
Insulation Material		XLPE
Nominal radial thickness	mm	12
Nominal diameter over insulation	mm	47.2
Insulation screen material(non metalic)		Extruded semi-conducting layer
Nominal radial thickness	mm	0.6
Swellable semi-conducting tape under metallic screen		Yes
Insulation screen (metalic)		CWS
No of wires × diameter	N×mm	60×1.04
Nominal tape thickness	mm/%	
C.S.A. (Cu wires)	mm^2	50
Swellable tape over metallic screen		Yes
Metallic / copolumer tape		Yes
Nominal total C.S.A.(Cu wires + Metallic / copolumer tape	mm^2	70
Outer sheath material		HDPE
Nominal radial thickness	mm	3
Nominal overall diameter	mm	58.8
Nominal total weight	kg/km	3585
Minimum bending radius	mm	804
Maximum conductor DC resistance, at 20°C	Ω/km	0.0778
Star reactance per phase, at 50Hz	Ω/km	0.133
Capacitance per phase	µF/km	0.180
Charging current, at U_o, 50Hz	A/km	2.374
Maximum permanent current rating in air/ground[a]	A	715/550
Maximum conductor temperature in service / in short-circuit	°C	90/250
Maximum adiabalic short-circuit current rating (0.1/0.5/1.0s)	kA	120/53.5/37.8

Table A.1: Data sheet handed out by Nyfors A/S.

[a] Cables in trefoil formation - cross bonded metallic screens - air, at 25°C / ground, at 15°C -1K·m/W - depth 1.3m

B CD contents

- Maps
    * Maps which shows the location of the cable.
- Measurements
    - Data jmkcur
    - Data jmkvol
    * Figures and data from the measurements.
- Nyfors AS - Documents handed out by Nyfors A/S.
    - Underdrillings
        * Drilling reports handed out by Nyfors A/S and calculation of average depth of underdrillings.
    * Calculation of ZPS impedance.
    * Data-sheet of cable
- References
    * Some of the sources referred in the report.
- Simulation models
    - Comsol
        - Result figures
        * Model of the PPS and ZPS test.
    - PSCAD
        - New model
            * The model with new parameters implemented.
        - Original model
            - Simulation results
            * The original model